Establishment of a Novel Ghrelin-Producing Cell Line

Hiroshi Iwakura, Yushu Li, Hiroyuki Ariyasu, Hiroshi Hosoda, Naotetsu Kanamoto, Mika Bando, Go Yamada, Kiminori Hosoda, Kazuwa Nakao, Kenji Kangawa, and Takashi Akamizu

Ghrelin Research Project (H.I., Y.L., H.A., M.B., T.A.), Translational Research Center, and Department of Medicine and Clinical Science, Endocrinology, and Metabolism (N.K., G.Y., K.H., K.N.), Kyoto University Hospital, Kyoto University Graduate School of Medicine, Kyoto 606-8507, Japan; and National Cardiovascular Center Research Institute (H.H., K.K.), Osaka 565-8565, Japan

To establish a tool to study ghrelin production and secretion *in vitro*, we developed a novel ghrelin-producing cell line, MGN3–1 (mouse ghrelinoma 3-1) cells from a gastric ghrelin-producing cell tumor derived from ghrelin-promoter Simian virus 40-T-antigen transgenic mice. MGN3-1 cells preserve three essential characteristics required for the *in vitro* tool for ghrelin research. First, MGN3-1 cells produce a substantial amount of ghrelin at levels approximately 5000 times higher than that observed in TT cells. Second, MGN3-1 cell expressed two key enzymes for acyl modification and maturation of ghrelin, namely ghrelin *O*-acyltransferase for acylation and prohormone convertase 1/3 for maturation and the physiological acyl modification and maturation of ghrelin were confirmed. Third, MGN3-1 cells retain physiological regulation of ghrelin secretion, at least in regard to the suppression by somatostatin and insulin, which is well established in *in vivo* studies. Thus, MGN3-1 cells are the first cell line derived from a gastric ghrelin-producing cell preserving secretion of substantial amounts of ghrelin under physiological regulation. This cell line will be a useful tool for both studying the production and secretion of ghrelin and screening of ghrelin-modulating drugs. (***Endocrinology* 151: 2940–2945, 2010)**

Ghrelin, a stomach-derived hormone, is composed of 28 amino acid residues with unique acyl-modification (1). Plasma ghrelin levels are regulated by acute and chronic energy status: serum levels are increased during a postprandial period and decreased after refeeding (2, 3). Ghrelin levels are low in obese individuals and high in lean people (4, 5). The direct factors regulating ghrelin secretion from ghrelin-producing cells (X/A-like cells), however, are not fully understood.

One method to investigate the direct effect of a specific factor on ghrelin secretion is to use a ghrelin-producing cell line. Ghrelin production has been reported by several cell lines, including TT (6), HL-60, THP-1, SupT1 (7), and HELL (8) cells. All of these cell lines differ completely from endogenous ghrelin-producing cells. TT cells originate from human thyroid medullary cancer, whereas HL-60, SupT1, and HELL cells are leukocyte in origin, with HELL being erythroleukemic line. Although these cell lines may be used to study ghrelin production (9), they are not ideal tools to study the regulation of ghrelin secretion. Therefore, establishment of a cell line originating from ghrelin-producing cells of the stomach would be useful for studying ghrelin production and secretion. Furthermore, it is vital to establish such cell line for studying factors directly affecting ghrelin production and secretion.

In this study, we established a ghrelin-producing cell line from a gastric tumor derived from ghrelin-promoter-Simian virus 40 T-antigen transgenic (GP-Tag Tg) mice.

Materials and Methods

Animals

GP-Tag Tg mice were generated as described previously (10). KSN nude mice were purchased from Shimizu Laboratory Supplies (Kyoto, Japan). Animals were maintained on

ISSN Print 0013-7227 ISSN Online 1945-7170
Printed in U.S.A.

doi: 10.1210/en.2010-0090 Received January 22, 2010. Accepted March 12, 2010.
First Published Online April 7, 2010

Abbreviations: AA, Amino acid; FBS, fetal bovine serum; GOAT, ghrelin *O*-acyltransferase; GP-Tag Tg, ghrelin-promoter-Simian virus 40 T-antigen transgenic; KRB, Krebs-Ringer buffer; PC, prohormone convertase; siRNA, small interfering RNA.

standard rodent food (CE-2, 352 kcal/100 g; Japan CLEA, Tokyo, Japan) on a 12-h light, 12-h dark cycle unless otherwise indicated. All experimental procedures were approved by the Kyoto University Graduate School of Medicine Committee on Animal Research.

Cell culture

A gastric tumor resected from a GP-Tag Tg mouse was minced and digested with the combination of 1.5 mg/ml collagenase type I (Sigma-Aldrich, St. Louis, MO) and 0.5 mg/ml dispase (Roche, Basel, Switzerland) in DMEM (11995-065; Life Technologies, Inc., Carlsbad, CA) supplemented with 10% fetal bovine serum (FBS) at 37 C for 90 min. After washing with PBS, tumor cells were cultured in DMEM supplemented with 10% FBS, 100 U/ml penicillin, and 100 μg/ml streptomycin at 37 C in 10% CO_2. Stromal cells were diminished by serial passage of tumor cells into new dishes 2–3 h after seeding the cells to the first dishes. After several passages of cells in 3-d intervals, the cells were cloned by dilution cloning onto a feeder layer of mitomycin-C-treated embryonic fibroblasts in 96-well microplates.

TT cells were cultured in Ham's F-12K supplemented with 10% FBS at 37 C in 5% CO_2 as described previously (6).

Immunocytochemistry

Cells were cultured in a chamber slide system (Nulge Nunc, Rochester, NY) and then fixed with 10% formalin for 15 min. Formalin-fixed slides were immunostained using the avidin-biotin peroxidase complex method (Vectastain ABC Elite kit; Vector Laboratories, Burlingame, CA) as described previously (11). Slides were incubated with anti-carboxy (C)-terminal ghrelin (amino acid, AA: 13-28) (12) (1:2000 at final dilution), which detects both ghrelin and desacyl-ghrelin, amino N-terminal ghrelin (12) that recognizes the *n*-octanoylated portion of ghrelin (AA: 1–11; 1:5000), antiglucagon (1:500) (Dako, Glostrup, Denmark), antisomatostatin (1:500) (Dako), and antigastrin (1:500) (Dako).

Electron microscope

Electron microscope study was performed as described previously (13). Cell pellets were fixed with 1% glutaraldehyde at 4 C for 2 h. After washing in phosphate buffer, samples were postfixed with 2% OsO_4 at 4 C for 2 h dehydrated with ethanol and embedded in Quetol 812 (Nisshin EM, Tokyo, Japan). Ultrathin sections of samples were cut, stained with uranyl acetate for 15 min followed by lead acetate for 5 min, and then viewed with an H-300 electron microscope (Hitachi, Tokyo, Japan).

Measurements of ghrelin concentrations in cells and culture medium

Cells were detached from dishes in enzyme-free cell dissociation buffer (Life Technologies). After centrifugation, cells were dissolved in PBS and boiled for 5 min. Acetic acid was added to each solution to a final concentration of 1 M. After needle shearing and centrifugation, the cell supernatants were applied to Sep-Pak C18 cartridges (Waters Corp., Milford, MA) preequilibrated with 0.9% saline. Cartridges were washed in saline and 5% CH_3CN/0.1% trifluoroacetic acid and eluted with 60% CH_3CN/0.1% trifluoroacetic acid. Eluates were lyophilized and subjected to ghrelin RIA. To measure ghrelin concentrations in culture medium, the collected culture media were centrifuged, and the resulting supernatants were immediately applied to Sep-Pak C18 cartridges and processed as described above. RIAs were performed using anti-C-terminal ghrelin (AA: 13–28) antiserum (C-RIA), which detects both ghrelin and desacyl-ghrelin, and anti-N-terminal ghrelin (AA: 1–11) antiserum (N-RIA), which detects ghrelin only, as described previously (12, 14).

RT-PCR and quantitative RT-PCR

Total RNA was extracted using a Sepasol-RNA kit (Nacalai Tesque, Kyoto, Japan). Reverse transcription was performed with a high-capacity cDNA reverse transcriptase kit (Applied Biosystems, Foster City, CA). RT-PCR was performed using a GeneAmp 9700 cycler (Applied Biosystems) with Amplitaqgold using appropriate primers (Supplemental Table 1 published on The Endocrine Society's Journals Online web site at http://endo.endojournals.org). Real-time quantitative PCR was performed using an ABI PRISM 7500 sequence detection system (Applied Biosystems) using appropriate primers and TaqMan probes or with Power SybrGreen (Supplemental Table 1). The mRNA expression of each gene was normalized to levels of 18S rRNA.

Western blotting

The molecular size of ghrelin in the medium was determined by tricine SDS-PAGE and Western blot analysis as described previously (10). MGN3-1 cells were seeded in 10-cm dishes (5.0×10^6 cells/dish). Culture media were collected after a 3-d incubation and subjected to HPLC purification and lyophilization as described above. Tricine SDS-PAGE and Western blot analysis were performed as described previously using anti-COOH-terminal ghrelin antibody (1:5000) (10).

Reverse-phase HPLC

MGN3-1 cells were seeded in a six-well dish (5×10^5 cells/well). After a washing in PBS, cells were incubated at 37 C for 4 h in DMEM supplemented with 0.5% BSA. Culture medium was collected and subjected to reverse-phase HPLC as described previously (6).

Small interfering RNA (siRNA)

Synthetic siRNAs and a negative control were purchased from Invitrogen (Carlsbad, CA). Two types of siRNAs specific for ghrelin *O*-acyltransferase (GOAT) were used: GCGCUUCUGUUUAAUUAUCUCUGCA (si1) and AGGAAGUCCAUAGGCUGACCUUCUU (si2). siRNAs were delivered into MGN3-1 cells using Lipofectamine RNAi Max (Invitrogen) according to the protocol provided by the manufacturer. The medium was changed after a 24-h incubation with siRNA. One mM of octanoic acid was added to the medium. Ghrelin levels in the media were measured after additional 6-d incubation.

Transplantation of MGN3-1 cells in nude mice

Eight-week-old male KSN nude mice were sc injected with 1.0×10^7 of MGN3-1 cells dissolved in PBS. Mice were housed individually with continuous access to chow and water. Food intake was measured by subtracting the remaining weight of the chow from that originally presented.

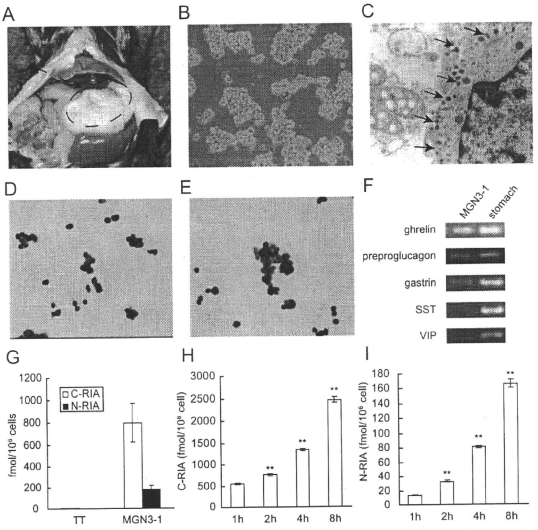

FIG. 1. Establishment of MGN3-1 cells A, Macroscopic findings of a ghrelinoma in a GP-Tag Tg mouse. B and C, Morphology of MGN3-1 cells by optic (B) and electron (C) microscopy. Secretory granules were observed (*arrow*). D and E, MGN3-1 cells were immunostained with anti-C-terminal ghrelin (D) and anti-N-terminal (E) ghrelin antibodies. F, RT-PCR analysis of the expression of mRNAs encoding gastric hormones in MGN3-1 cells. SST, Somatostatin; VIP, vasoactive intestinal polypeptide. G, Ghrelin peptide content determined by C-RIA and N-RIA in TT and MGN3-1 cells. H and I, Time course changes of ghrelin levels in the medium in which MGN3-1 cells were incubated. **, $P < 0.01$ compared with 1 h ($n = 9$).

Measurements of plasma ghrelin concentrations

Plasma samples were collected as reported previously (10). Plasma ghrelin and desacyl ghrelin concentrations were determined using an active ghrelin ELISA kit that recognizes *n*-octanoylated ghrelin and a desacyl ghrelin ELISA kit (both from Mitsubishi Kagaku Iatron, Tokyo, Japan), respectively (15).

Batch incubation study

MGN3-1 cells were seeded and cultured overnight in 12-well plates (7.5×10^5 cells/well). After a washing in PBS, cells were incubated at 37 C for 4 h in DMEM or Krebs-Ringer buffer (KRB) supplemented with 0.5% BSA and the indicated additional reagents (octanoic acid, somatostatin, or insulin) before collecting supernatants. Ghrelin concentrations in the supernatant were measured by RIA as described above. To determine the expression levels of ghrelin and GOAT mRNA, cells were incubated at 37 C for 24 h in DMEM supplemented with 0.5% BSA and the indicated additional reagents.

Statistical analysis

All values were expressed as the means ± SE. The statistical significance of the differences in mean values was assessed by ANOVA with a *post hoc* test (Tukey's test) or Student's *t* test as appropriate. Difference with $P < 0.05$ was considered significant.

Results

Establishment of MGN3-1 cell line

GP-Tag Tg mice (10) develop gastric tumors (Fig. 1A), which produce and secrete ghrelin and preserving the physiological regulation, at least by feeding status, sex difference, and body weights *in vivo*. We established a cell line, MGN3-1 cell, from a gastric tumor derived from a GP-Tag Tg mouse (Fig. 1A). MGN3-1 cells formed round-shaped aggregates that stuck together with moderate adhesion to culture dishes (Fig. 1B). These cells contained secretory granules when observed by electron microscopy (Fig. 1C). MGN3-1 cells exhibited ghrelin-like immunoreactivity by immunocytochemistry using anti-N-terminal, which recognizes ghrelin only, and anti-C-terminal ghrelin, which recognizes both ghrelin and desacyl ghrelin, antibodies (Fig. 1, D and E). We found the production of ghrelin mRNA by MGN3-1 cells using RT-PCR (Fig. 1F). This method also detected low levels of preproglucagon and gastrin mRNA (Fig. 1F) in MGN3-1 cells, whereas immunostaining with antiglucagon and antigastrin antibodies could not detect any expression of these proteins (data not shown). No expression of somatostatin and vasoactive intestinal polypeptide mRNA was observed in MGN3-1 cell (Fig. 1F). MGN3-1 cells contained approximately 140-fold higher levels of total ghrelin (*n*-octanoylated ghrelin plus desacyl ghrelin) measured by C-RIA and approximately 5000-fold higher levels of ghrelin measured by N-RIA than those observed in TT cells (Fig. 1G). The ghrelin levels in the medium were increased time dependently when MGN3-1 cells were incubated in DMEM (Fig. 1, H and I).

Acyl modification and maturation of ghrelin in MGN3-1 cells

MGN3-1 cells expressed GOAT, prohormone convertase (PC) 1/3 and PC2 mRNA (Fig. 2A). The molecular size of ghrelin examined by tricine SDS-PAGE and Western blot analysis in culture medium was consistent with that of mature ghrelin (Fig. 2B). In addition, when the culture

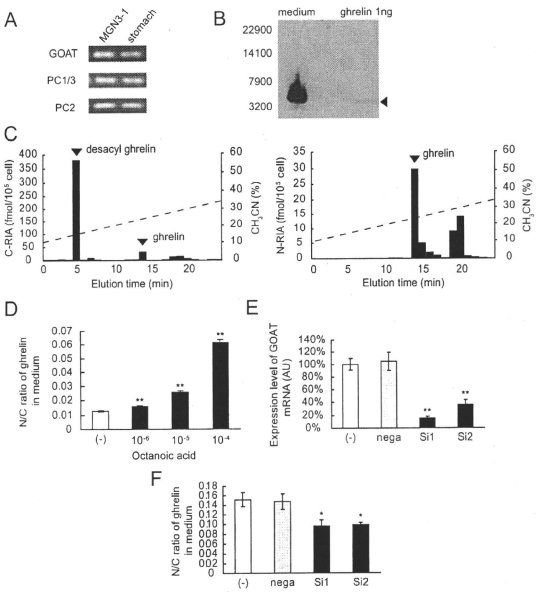

FIG. 2. Acylation and processing of ghrelin in MGN3-1 cells. A, RT-PCR analysis of GOAT, PC1/3, and PC2 mRNA expressions in MGN3-1 cells. B, Western blot analysis of culture medium in which MGN3-1 cells were cultured for 3 d. Rat ghrelin peptide was used as a positive control. C, Representative reverse-phase HPLC profiles of ghrelin immunoreactivity in the medium in which MGN3-1 cells were cultured for 4 h. D, The ratio of N-RIA to C-RIA of ghrelin secreted by MGN3-1 cells incubated for 4 h in KRB supplemented with 0.5% BSA and various concentrations of octanoic acid. **, $P < 0.01$ in comparison with (−) (n = 9). E, GOAT mRNA levels after siRNA treatment of MGN3-1 cells. Two types of siRNA specific for GOAT (Si1 and Si2) and negative control (nega) were introduced into MGN3-1 cell. *, $P < 0.05$, **, $P < 0.01$ in comparison with (−) (n = 7). AU, Arbitrary unit. F, The ratio of N-RIA to C-RIA of ghrelin secreted by MGN3-1 cells after siRNA treatment. *, $P < 0.05$, **, $P < 0.01$ in comparison with (−) (n = 7).

Transplantation of MGN3-1 cell to nude mouse

When MGN3-1 cells were injected sc into nude mice, they developed solid tumors (Fig. 3A). Plasma ghrelin and desacyl ghrelin levels were significantly elevated in nude mice 4 wk after MGN3-1 cell injection (Fig. 3, B and C). Mice injected with MGN3-1 cells exhibited significantly higher food intake in comparison with controls (PBS *vs.* cell: 21.4 ± 0.5 *vs.* 23.3 ± 0.7 g/wk, $P < 0.05$) 4 wk after injection (Fig. 3C).

The effect of somatostatin and insulin on ghrelin secretion and expression *in vitro*

MGN3-1 cells expressed the mRNAs encoding multiple somatostatin receptors, primarily type 2 and 5 with lower levels of type 3 and 4 (Fig. 4A). When somatostatin was added to culture media, ghrelin secretion was suppressed in a dose-dependent manner (Fig. 4, B and C). MGN3-1 cells also expressed mRNA of insulin receptor (Fig. 4A). Addition of insulin to culture media also suppressed ghrelin secretion from MGN3-1 cell (Fig. 4, D and E). Somatostatin treatment did not affect mRNA expression of either ghrelin or GOAT, even for 24 h incubation (Fig. 4, F and G), whereas insulin significantly suppressed them (Fig. 4, H and I).

media were subjected to reverse-phase HPLC, the immunoreactive peaks detected by C-RIA and N-RIA were eluted at the positions identical with those of desacyl ghrelin and ghrelin (Fig. 2C). When MGN3-1 cells were incubated in KRB supplemented with 0.5% BSA, addition of octanoic acid to KRB significantly increased the ratio of *n*-octanoylated ghrelin measured by N-RIA to total ghrelin measured by C-RIA (N to C ratio) (Fig. 2D). Specific siRNA1 and siRNA2 treatment decreased GOAT mRNA levels in MGN3-1 cells to 85 and 65% of normal levels, respectively (Fig. 2E). The N to C ratio was significantly decreased by GOAT knockdown (Fig. 2F), indicating that GOAT mediates the acylation of ghrelin in MGN3-1 cells.

Discussion

In this study, we successfully established the first ghrelinoma cell line, MGN3-1 cell. When establishing a cell line for a research tool, the most important thing is how the established cell line keeps its original characteristics. We evaluated the value of MGN3-1 cell by three points: the quantity of ghrelin production, the maintenance of machineries involved in acyl modification and maturation of ghrelin, and the preservation of known *in vivo* regulation of ghrelin secretion.

With regard to the amount of ghrelin production, MGN3-1 cells produced substantial quantities of ghrelin, approximately 5000-fold greater than that produced by

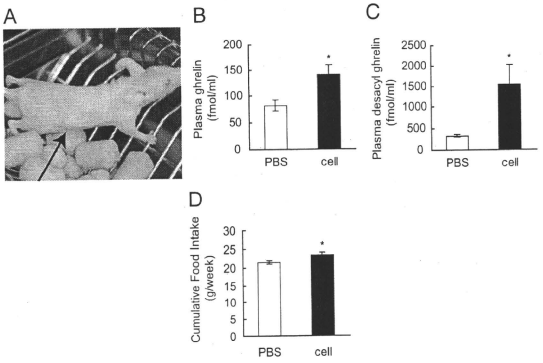

FIG. 3. Transplantation of MGN3-1 cell to nude mouse. A, Macroscopic findings of nude mice injected with MGN3-1 cells. B and C, Plasma ghrelin (B) and desacyl ghrelin (C) levels in nude mice at 4 wk after injection of saline or MGN3-1 cells. D, Cumulative food intake over a week (between 4 and 5 wk after injection) by mice injected with MGN3-1 cells (cell) or PBS. *, $P < 0.05$ in comparison with PBS ($n = 5$).

TT cells (6). It may be reasonable because TT cell is originated from thyroid medullary carcinoma, not from gastric ghrelin-producing cells. As for the machinery of ghrelin acyl modification and maturation, the MGN3-1 cell expressed two key enzymes: GOAT for acylation (16) and PC1/3 for processing (17). We confirmed the activity of GOAT in the MGN3-1 cell by the experiment in which the ratio of ghrelin to total ghrelin levels was decreased by knocking down the GOAT in MGN3-1 cells. Furthermore, addition of octanoic acid significantly increased the N to C ratio of ghrelin in the medium, which is consistent with the *in vivo* finding by Nishi *et al.* (18). We consider these findings important because acyl modification of ghrelin is one of the targets of drug discovery. On the other hand, tricine-SDS PAGE followed by Western blot analysis and reverse-phase HPLC confirmed the maturation of ghrelin in MGN3-1 cells. To provide a concrete evidence for the ability of producing bioactive ghrelin of MGN 3-1 cells, we performed a transplantation of MGN3-1 cells to nude mice, which resulted in the increase in plasma ghrelin levels and the enhancement of food intake in the nude mice. These results indicate that MGN3-1 cell keeps the ability to produce a substantial amount of bioactive ghrelin with normal acyl modification and maturation.

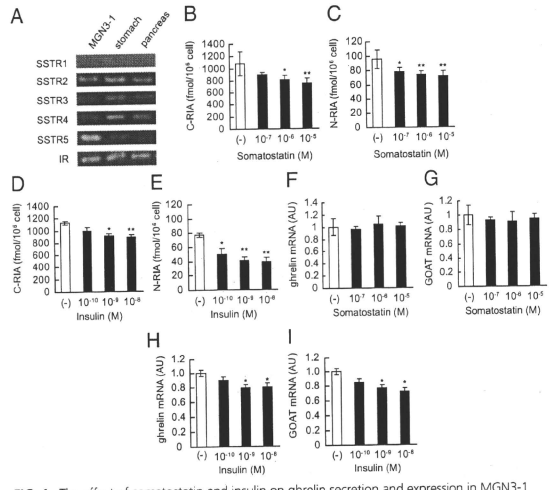

FIG. 4. The effect of somatostatin and insulin on ghrelin secretion and expression in MGN3-1 cells. A, RT-PCR analysis of somatostatin receptor (SSTR) types 1–5 and insulin receptor (IR) mRNA expressions in MGN3-1 cells. B–F, Ghrelin secretion was suppressed when MGN3-1 cells were incubated in DMEM supplemented with somatostatin (B and C) or insulin (D and E) for 4 h ($n = 6$). F–I, Somatostatin did not affect the expression levels of ghrelin (F) and GOAT (G) mRNA in MGN3-1 cell after 24 h incubation, whereas insulin significantly suppressed the expression levels of ghrelin (H) and GOAT (I) mRNA ($n = 6$). AU, Arbitrary unit. *, $P < 0.05$, **, $P < 0.01$ in comparison with (–).

Lastly, we examined the effect of a factor known to effect ghrelin secretion *in vivo*. Numerous reports exist examining the factors that regulate ghrelin secretion *in vivo* (19–27). Among those, the suppression of ghrelin secretion by somatostatin (19–22) or insulin (28, 29) is well established. We confirmed that ghrelin secretion is suppressed by somatostatin and insulin in MGN3-1 cells, indicating that MGN3-1 cells preserves the intrinsic characteristics of ghrelin-producing cells, at least with regard to its regulation by somatostatin and insulin.

In summary, we have established the first ghrelinoma cell line MGN3-1. The MGN3-1 cell line produces high amounts of bioactive ghrelin with normal acyl modification and maturation and retains physiological regulation by somatostatin. MGN3-1 will be a useful tool for

studying ghrelin production and secretion as well as for screening of ghrelin-modulating drugs.

Acknowledgments

We thank Ms. Chieko Ishimoto and Ms. Chinami Shiraiwa for their excellent technical assistance.

Address all correspondence and requests for reprints to: Hiroshi Iwakura, M.D., Ph.D., 54 Shogoin Kawahara-cho, Sakyo-ku, Kyoto 606-8507, Japan. E-mail: hiwaku@kuhp.kyoto-u.ac.jp.

This work was supported by funds from the Ministry of Education, Culture, Sports, Science, and Technology of Japan and the Ministry of Health, Labor, and Welfare of Japan.

Disclosure Summary: All authors have nothing to declare.

References

1. Kojima M, Hosoda H, Date Y, Nakazato M, Matsuo H, Kangawa K 1999 Ghrelin is a growth-hormone-releasing acylated peptide from stomach. Nature 402:656–660
2. Cummings DE, Purnell JQ, Frayo RS, Schmidova K, Wisse BE, Weigle DS 2001 A preprandial rise in plasma ghrelin levels suggests a role in meal initiation in humans. Diabetes 50:1714–1719
3. Tschöp M, Wawarta R, Riepl RL, Friedrich S, Bidlingmaier M, Landgraf R, Folwaczny C 2001 Post-prandial decrease of circulating human ghrelin levels. J Endocrinol Invest 24:RC19–RC21
4. Tschöp M, Weyer C, Tataranni PA, Devanarayan V, Ravussin E, Heiman ML 2001 Circulating ghrelin levels are decreased in human obesity. Diabetes 50:707–709
5. Ariyasu H, Takaya K, Tagami T, Ogawa Y, Hosoda K, Akamizu T, Suda M, Koh T, Natsui K, Toyooka S, Shirakami G, Usui T, Shimatsu A, Doi K, Hosoda H, Kojima M, Kangawa K, Nakao K 2001 Stomach is a major source of circulating ghrelin, and feeding state determines plasma ghrelin-like immunoreactivity levels in humans. J Clin Endocrinol Metab 86:4753–4758
6. Kanamoto N, Akamizu T, Hosoda H, Hataya Y, Ariyasu H, Takaya K, Hosoda K, Saijo M, Moriyama K, Shimatsu A, Kojima M, Kangawa K, Nakao K 2001 Substantial production of ghrelin by a human medullary thyroid carcinoma cell line. J Clin Endocrinol Metab 86:4984–4990
7. De Vriese C, Delporte C 2007 Autocrine proliferative effect of ghrelin on leukemic HL-60 and THP-1 cells. J Endocrinol 192:199–205
8. De Vriese C, Grégoire F, De Neef P, Robberecht P, Delporte C 2005 Ghrelin is produced by the human erythroleukemic HEL cell line and involved in an autocrine pathway leading to cell proliferation. Endocrinology 146:1514–1522
9. Gutierrez JA, Solenberg PJ, Perkins DR, Willency JA, Knierman MD, Jin Z, Witcher DR, Luo S, Onyia JE, Hale JE 2008 Ghrelin octanoylation mediated by an orphan lipid transferase. Proc Natl Acad Sci USA 105:6320–6325
10. Iwakura H, Ariyasu H, Li Y, Kanamoto N, Bando M, Yamada G, Hosoda H, Hosoda K, Shimatsu A, Nakao K, Kangawa K, Akamizu T 2009 A mouse model of ghrelinoma exhibited activated growth hormone-insulin-like growth factor I axis and glucose intolerance. Am J Physiol Endocrinol Metab 297:E802–E811
11. Iwakura H, Hosoda K, Doi R, Komoto I, Nishimura H, Son C, Fujikura J, Tomita T, Takaya K, Ogawa Y, Hayashi T, Inoue G, Akamizu T, Hosoda H, Kojima M, Kangawa K, Imamura M, Nakao K 2002 Ghrelin expression in islet cell tumors: augmented expression of ghrelin in a case of glucagonoma with multiple endocrine neoplasm type I. J Clin Endocrinol Metab 87:4885–4888
12. Hosoda H, Kojima M, Matsuo H, Kangawa K 2000 Ghrelin and des-acyl ghrelin: two major forms of rat ghrelin peptide in gastrointestinal tissue. Biochem Biophys Res Commun 279:909–913
13. Iwakura H, Ariyasu H, Kanamoto N, Hosoda K, Nakao K, Kangawa K, Akamizu T 2008 Establishment of a novel neuroblastoma mouse model. Int J Oncol 33:1195–1199
14. Iwakura H, Hosoda K, Son C, Fujikura J, Tomita T, Noguchi M, Ariyasu H, Takaya K, Masuzaki H, Ogawa Y, Hayashi T, Inoue G, Akamizu T, Hosoda H, Kojima M, Itoh H, Toyokuni S, Kangawa K, Nakao K 2005 Analysis of rat insulin II promoter-ghrelin transgenic mice and rat glucagon promoter-ghrelin transgenic mice. J Biol Chem 280:15247–15256
15. Akamizu T, Shinomiya T, Irako T, Fukunaga M, Nakai Y, Kangawa K 2005 Separate measurement of plasma levels of acylated and desacyl ghrelin in healthy subjects using a new direct ELISA. J Clin Endocrinol Metab 90:6–9
16. Yang J, Brown MS, Liang G, Grishin NV, Goldstein JL 2008 Identification of the acyltransferase that octanoylates ghrelin, an appetite-stimulating peptide hormone. Cell 132:387–396
17. Zhu X, Cao Y, Voogd K, Voogd K, Steiner DF 2006 On the processing of proghrelin to ghrelin. J Biol Chem 281:38867–38870
18. Nishi Y, Hiejima H, Hosoda H, Kaiya H, Mori K, Fukue Y, Yanase T, Nawata H, Kangawa K, Kojima M 2005 Ingested medium-chain fatty acids are directly utilized for the acyl modification of ghrelin. Endocrinology 146:2255–2264
19. Shimada M, Date Y, Mondal MS, Toshinai K, Shimbara T, Fukunaga K, Murakami N, Miyazato M, Kangawa K, Yoshimatsu H, Matsuo H, Nakazato M 2003 Somatostatin suppresses ghrelin secretion from the rat stomach. Biochem Biophys Res Commun 302:520–525
20. Silva AP, Bethmann K, Raulf F, Schmid HA 2005 Regulation of ghrelin secretion by somatostatin analogs in rats. Eur J Endocrinol 152:887–894
21. Norrelund H, Hansen TK, Orskov H, Hosoda H, Kojima M, Kangawa K, Weeke J, Moller N, Christiansen JS, Jorgensen JO 2002 Ghrelin immunoreactivity in human plasma is suppressed by somatostatin. Clin Endocrinol (Oxf) 57:539–546
22. Broglio F, Koetsveld Pv P, Benso A, Gottero C, Prodam F, Papotti M, Muccioli G, Gauna C, Hofland L, Deghenghi R, Arvat E, Van Der Lely AJ, Ghigo E 2002 Ghrelin secretion is inhibited by either somatostatin or cortistatin in humans. J Clin Endocrinol Metab 87:4829–4832
23. Sugino T, Yamaura J, Yamagishi M, Kurose Y, Kojima M, Kangawa K, Hasegawa Y, Terashima Y 2003 Involvement of cholinergic neurons in the regulation of the ghrelin secretory response to feeding in sheep. Biochem Biophys Res Commun 304:308–312
24. Broglio F, Gottero C, Van Koetsveld P, Prodam F, Destefanis S, Benso A, Gauna C, Hofland L, Arvat E, van der Lely AJ, Ghigo E 2004 Acetylcholine regulates ghrelin secretion in humans. J Clin Endocrinol Metab 89:2429–2433
25. Grinspoon S, Miller KK, Herzog DB, Grieco KA, Klibanski A 2004 Effects of estrogen and recombinant human insulin-like growth factor-I on ghrelin secretion in severe undernutrition. J Clin Endocrinol Metab 89:3988–3993
26. Koutkia P, Canavan B, Breu J, Johnson ML, Grinspoon SK 2004 Nocturnal ghrelin pulsatility and response to growth hormone secretagogues in healthy men. Am J Physiol Endocrinol Metab 287:E506–E512
27. Basa NR, Wang L, Arteaga JR, Heber D, Livingston EH, Taché Y 2003 Bacterial lipopolysaccharide shifts fasted plasma ghrelin to postprandial levels in rats. Neurosci Lett 343:25–28
28. Murdolo G, Lucidi P, Di Loreto C, Parlanti N, De Cicco A, Fatone C, Fanelli CG, Bolli GB, Santeusanio F, De Feo P 2003 Insulin is required for prandial ghrelin suppression in humans. Diabetes 52:2923–2927
29. Saad MF, Bernaba B, Hwu CM, Jinagouda S, Fahmi S, Kogosov E, Boyadjian R 2002 Insulin regulates plasma ghrelin concentration. J Clin Endocrinol Metab 87:3997–4000

Available online at www.sciencedirect.com
ScienceDirect
Metabolism Clinical and Experimental 59 (2010) 1241 – 1251
Metabolism
Clinical and Experimental
www.metabolismjournal.com

Adipose tissue–specific dysregulation of angiotensinogen by oxidative stress in obesity

Sadanori Okada[a,b,1], Chisayo Kozuka[a,1], Hiroaki Masuzaki[a,*], Shintaro Yasue[a], Takako Ishii-Yonemoto[a], Tomohiro Tanaka[a], Yuji Yamamoto[a], Michio Noguchi[a], Toru Kusakabe[a], Tsutomu Tomita[a], Junji Fujikura[a], Ken Ebihara[a], Kiminori Hosoda[a], Hiroshi Sakaue[c], Hiroyuki Kobori[d], Mira Ham[e], Yun Sok Lee[e], Jae Bum Kim[e], Yoshihiko Saito[b], Kazuwa Nakao[a]

[a]*Department of Medicine and Clinical Science, Kyoto University Graduate School of Medicine, Kyoto 606-8507, Japan*
[b]*First Department of Internal Medicine, Nara Medical University, Kashihara 634-8522, Japan*
[c]*Department of Nutrition and Metabolism, Institute of Health Biosciences, The University of Tokushima Graduate School, Tokushima 770-8503, Japan*
[d]*Departments of Medicine and Physiology, and Hypertension and Renal Center of Excellence, Tulane University Health Sciences Center, New Orleans, LA 70112-2699, USA*
[e]*Institute of Molecular Biology and Genetics, Seoul National University, Seoul 110-744, South Korea*

Received 27 August 2009; accepted 18 November 2009

Abstract

Adipose tissue expresses all components of the renin-angiotensin system including angiotensinogen (AGT). Recent studies have highlighted a potential role of AGT in adipose tissue function and homeostasis. However, some controversies surround the regulatory mechanisms of AGT in obese adipose tissue. In this context, we here demonstrated that the AGT messenger RNA (mRNA) level in human subcutaneous adipose tissue was significantly reduced in obese subjects as compared with nonobese subjects. Adipose tissue AGT mRNA level in obese mice was also lower as compared with their lean littermates; however, the hepatic AGT mRNA level remained unchanged. When 3T3-L1 adipocytes were cultured for a long period, the adipocytes became hypertrophic with a marked increase in the production of reactive oxygen species. Expression and secretion of AGT continued to decrease during the course of adipocyte hypertrophy. Treatment of the 3T3-L1 and primary adipocytes with reactive oxygen species (hydrogen peroxide) or tumor necrosis factor α caused a significant decrease in the expression and secretion of AGT. On the other hand, treatment with the antioxidant *N*-acetyl cysteine suppressed the decrease in the expression and secretion of AGT in the hypertrophied 3T3-L1 adipocytes. Finally, treatment of obese *db/db* mice with *N*-acetyl cysteine augmented the expression of AGT in the adipose tissue, but not in the liver. The present study demonstrates for the first time that oxidative stress dysregulates AGT in obese adipose tissue, providing a novel insight into the adipose tissue–specific interaction between the regulation of AGT and oxidative stress in the pathophysiology of obesity.

1. Introduction

Overactivity of the systemic renin-angiotensin system (RAS) is one of the central mechanisms for obesity-related metabolic disorders [1,2]. Notably, the major components of the RAS are expressed in various tissues including the heart, blood vessels, adipose tissue, and brain [3]; these comprise tissue RAS. A series of products are produced locally from

The authors of this manuscript have nothing to declare.

Institutional approval: The human study was approved by the ethics committee for human research of the Kyoto University Graduate School of Medicine (2004, no. 553). Written informed consent was obtained from all subjects prior to the study. All animal experimental procedures were approved by the Kyoto University Graduate School of Medicine Animal Research Committee and the Seoul National University Animal Experiment Ethics Committee.

* Corresponding author. Division of Endocrinology and Metabolism, Second Department of Internal Medicine, Faculty of Medicine, University of the Ryukyus, Okinawa 903-0215, Japan. Tel.: +81 98 895 1145; fax: +81 98 895 1415.
E-mail address: hiroaki@med.u-ryukyu.ac.jp (H. Masuzaki).

[1] Sadanori Okada and Chisayo Kozuka contributed equally to this work.

0026-0495/$ – see front matter © 2010 Elsevier Inc. All rights reserved.
doi:10.1016/j.metabol.2009.11.016

angiotensinogen (AGT), the unique precursor of angiotensin peptides, and play a critical role in cardiovascular homeostasis [3,4].

Although AGT is produced mainly by the liver, adipose tissue is also considered as a source of AGT production [5]. In agreement with this notion, the adipose tissue expresses all components of the RAS, including AGT, renin, angiotensin I–converting enzyme, and angiotensin II type 1 receptor, in humans and rodents [6,7]. A previous study has demonstrated that AGT-deficient mice are low in blood pressure and body fat mass [8]. Moreover, adipocyte-specific transgenic overexpression of AGT on an AGT-deficient background was shown to augment plasma AGT level and rescue hypotension and leanness [9]. These results indicate that adipose tissue–derived AGT does contribute to the circulating AGT level and adipogenesis.

In rodent experiments, the AGT messenger RNA (mRNA) level in white adipose tissue has been shown to be regulated by the nutritional status; however, that in the liver was independent of the nutritional status [10,11]. In human cross-sectional studies, the AGT mRNA level in adipose tissue was shown to be higher in obese subjects [6,12]. On the other hand, another study reported that the AGT mRNA level in adipose tissue was significantly lower in obese individuals [13]. Elevation of AGT expression in adipose tissue in obese individuals thus remains controversial [14].

Several studies have shown that increased oxidative stress is a manifestation of obesity-related metabolic derangement [15-17]. In fact, in humans, oxidative stress is critically associated with atherosclerosis, hypertension, and diabetes mellitus [18,19]. Oxidative stress is also related with the RAS. Angiotensin II is a potent inducer of reactive oxygen species (ROS) in a variety of tissues [20-22]. In the liver and kidney, increased ROS has been reported to increase AGT gene expression [23-26]. Also in obese adipose tissue, generation of ROS is exaggerated and is involved in adipose tissue dysfunction [17,27]. However, whether increased ROS may affect adipose AGT production remains to be elucidated.

In the present study, we demonstrated that the AGT mRNA level was reduced in obese adipose tissue in humans and mice and in hypertrophied 3T3-L1 adipocytes. In this context, we tested the hypothesis that increased oxidative stress would modulate AGT in obese adipose tissue.

2. Materials and methods

2.1. Subcutaneous abdominal adipose tissue biopsies in human subjects

The present study was performed according to the Declaration of Helsinki and approved by the Ethical Committee on Human Research of Kyoto University Graduate School of Medicine (2004, no. 553). Written informed consent was obtained from all subjects before the study.

Subcutaneous abdominal adipose tissue biopsies were obtained from 46 Japanese subjects (24 men and 22 women; age [mean ± SD], 46 ± 2.1 years). The body mass index (BMI) of the subjects ranged from 19 to 52 (mean ± SD, 30 ± 1.6) kg/m^2. All subjects had been on stable therapy with lipid-lowering, antihypertensive, or hypoglycemic agents for at least 1 month before admission and continued with the same doses throughout the study period. Patients who received angiotensin I–converting enzyme inhibitors, angiotensin II receptor blockers, and steroid-related drugs were carefully excluded. For the study, subcutaneous abdominal adipose depots of the study subjects were excised from the periumbilical region under local anesthesia. The samples were immediately frozen in liquid nitrogen and stored at −80°C until use.

2.2. Mouse experiments

Male *ob/ob* mice (age, 12 weeks) were purchased from Oriental BioService (Kyoto, Japan) and housed in the animal facility of Kyoto University. Male *db/db* mice (age, 10 weeks) were purchased from Japan SLC (Hamamatsu, Japan) and housed in Seoul National University. The mice were allowed free access to food and water. For in vivo antioxidant treatment, the *db/db* mice were injected with *N*-acetyl cysteine (NAC; 150 mg/kg body weight; Sigma-Aldrich Japan, Tokyo, Japan) or the vehicle (phosphate-buffered saline) into the peritoneal cavity once daily for 1 week. All experimental procedures were approved by the Kyoto University Graduate School of Medicine Animal Research Committee and the Seoul National University Animal Experiment Ethics Committee.

2.3. Cell culture and isolation of primary adipocytes

3T3-L1 fibroblasts were cultured and differentiated into adipocytes as described previously [28]. Briefly, the 2-day postconfluent cells (designated as day 0) were incubated for 2 days with 10% fetal bovine serum (FBS)/Dulbecco modified Eagle medium (DMEM), 0.5 mmol/L 3-isobutyl-1-methylxanthine, 0.25 μmol/L dexamethasone, and 1 μg/mL insulin. The cells were then incubated for 2 days in 10% FBS/DMEM with insulin and, thereafter, incubated in 10% FBS/DMEM that was changed on every alternate day. Oil red O staining was performed as described [29].

Primary adipocytes were isolated from epididymal fat pads of 9-week-old male C57BL/6J mice (purchased from Oriental BioService, Kyoto, Japan). Epididymal fat pads were harvested, minced into 2- to 3-mm pieces, and digested using 0.8 mg/mL collagenase (Sigma-Aldrich Japan) in DMEM for 30 minutes at 37°C in a shaking water bath. After the digestion with collagenase, cells were filtered through a 250-μm nylon filter and centrifuged at 1000 rpm for 30 seconds. The suspended mature adipocytes were separated from the pelleted stromovascular fraction and washed 3 times in DMEM for experiments.

2.4. Determination of adipocyte size

The cells were fixed with 2% osmium tetroxide and passed through a 250-μm nylon filter to remove the fibrous elements, and the cells were washed extensively with isotonic saline. A total of 10 000 cells was analyzed using the Coulter Multisizer III (Beckman Coulter, High Wycombe, England) [30].

2.5. Quantitative real-time polymerase chain reaction

Total RNA was extracted from human and mouse adipose tissue by using a QIAGEN RNeasy Mini Kit (QIAGEN Japan, Tokyo, Japan) and from cultured adipocytes by using Trizol Reagent (Invitrogen, Carlsbad, CA). Complementary DNA was then synthesized by using an iScript cDNA Synthesis Kit (Bio-Rad, Hercules, CA). Taqman polymerase chain reactions (PCRs) for human AGT, mouse AGT, mouse monocyte chemoattractant protein 1 (MCP-1), mouse interleukin 6 (IL-6), and mouse tumor necrosis factor α (TNFα) were performed using the ABI Prism 7300 Sequence Detection System (Applied Biosystems, Foster City, CA). The sequences of probes and primers are summarized in Table 1.

2.6. Enzyme-linked immunosorbent assay

The AGT protein level in the culture media was measured by sandwich-type enzyme-linked immunosorbent assay (ELISA) as described [31]. Similarly, the MCP-1 and IL-6 protein levels were detected by using an ELISA kit (R&D Systems, Minneapolis, MN).

2.7. Determination of ROS

The ROS activity was determined by the nitroblue tetrazolium (NBT) assay [32]. Reduced NBT (formazan) was dissolved in 50% acetic acid, and the absorbance of the supernatant was determined at 560 nm.

2.8. Statistical analysis

The data are presented as the mean ± SE. Unpaired Student t test was used for comparisons with the control group. The differences were accepted as significant at a level of $P < .05$.

3. Results

3.1. AGT mRNA expression level in adipose tissue from obese humans and mice

To explore the impact of obesity on AGT gene expression in human adipose tissue, we performed subcutaneous abdominal adipose tissue biopsies from 46 subjects with a wide range of BMI. The AGT mRNA level was significantly reduced by 61% in the obese subjects as compared with the nonobese subjects (Fig. 1A).

To verify the obesity-related decrease in adipose AGT expression, we analyzed adipose tissue from genetically obese mice. In 12-week-old male *ob/ob* mice (mean body weight, 60 ± 0.7 g), the AGT mRNA level was significantly decreased in both epididymal (29%) and subcutaneous (57%) adipose depots as compared with their lean littermates (mean body weight, 29 ± 0.3 g) (Fig. 1B). On the other hand, the AGT mRNA levels in the liver remained unaltered in both groups (Fig. 1C).

Similar results were observed in case of the diet-induced obese (DIO) mice (12-week-old male C57BL/6J mice fed with a high-fat/high-sucrose diet for 4 weeks). The AGT mRNA level in the adipose tissue of the DIO mice (mean body weight, 40 ± 0.8 g) was significantly lower than that in the adipose tissue of their lean littermates (mean body weight, 30 ± 0.4 g) ($P < .05$); however, the hepatic AGT mRNA level remained unchanged in both groups (Yasue et al, unpublished observations). These results indicate that the AGT mRNA level was decreased exclusively in the obese adipose tissue in both humans and mice.

3.2. AGT expression during the course of hypertrophy in the 3T3-L1 adipocytes

To explore the mechanism by which AGT is decreased in obese adipose tissue, we analyzed hypertrophied adipocytes. 3T3-L1 fibroblasts were completely differentiated into

Table 1
Sequences of Taqman PCR primers and probes

Gene name Genbank accession no.	Forward primer Reverse primer	Probe (5′-FAM, 3′-TAMRA)
Human AGT NM_000029	GGTGGAGGGTCTCACTTTCCA ATGGTCAGGTGGATGGTCCG	CCCTCAACTGGATGAAGAAACTGTCTCC
Mouse Agt NM_007428	ACACCTACGTTCACTTCCAAG CCGAGATGCTGTTGTCCAC	ATGAGAGGTTTCTCTCAGCTGCCTGGA
Mouse Ccl2 (MCP-1) NM_011333	TTGGCTCAGCCAGATGC CCAGCCTACTCATTGGGATCA	CCCCACTCACCTGCTGCTACTCATTCA
Mouse Il6 (IL-6) NM_031168	ATGAAGTTCCTCTCTGCAAGAG GTAGGGAAGGCCGTGGTTG	CACCAGCATCAGTCCCAAGAAGGCA
Mouse Tnf (TNFα) NM_013693	TCTCTTCAAGGGACAAGGCTG ATAGCAAATCGGCTGACGGT	CCCGACTACGTGCTCCTCACCCA

The sequences of primers and probes for each gene used in the present study are summarized.

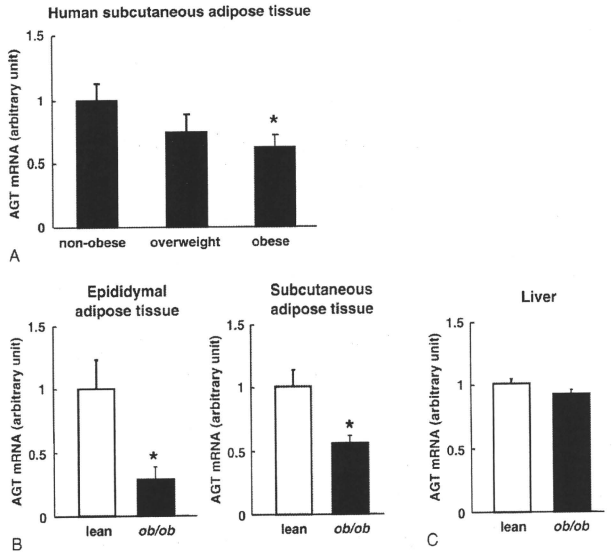

Fig. 1. The AGT mRNA levels in obese adipose tissue from humans and mice. A, The relation between the AGT mRNA level in subcutaneous abdominal adipose tissue and the degree of obesity in humans: nonobese (BMI <25), n = 20; overweight (25 ≤ BMI < 30), n = 13; obese (BMI ≥30), n = 13. B, Comparison of the adipose tissue AGT mRNA levels in 12-week-old male *ob/ob* mice (n = 4; mean body weight, 60 ± 0.7 g) and their lean littermates (n = 4; mean body weight, 29 ± 0.3 g). Left: epididymal adipose tissue depots. Right: subcutaneous abdominal adipose tissue depots. C, Comparison of the hepatic AGT mRNA level between the *ob/ob* mice (n = 4) and their lean littermates (n = 4). The mRNA level was examined by real-time PCR and normalized to that of 18S ribosomal RNA (rRNA). The data are expressed as the mean ± SE. **P* < .05 as compared with the nonobese subjects or the lean littermates.

adipocytes for 8-day incubation with induction media [28]. Consistent with a previous report [33], the AGT mRNA level in differentiated 3T3-L1 adipocytes (day 8) was significantly elevated by 15-folds in comparison with 3T3-L1 fibroblasts (day 0). For generating hypertrophied adipocytes, 3T3-L1 adipocytes were cultured up to 30 days after the induction of differentiation. Oil red O staining exhibited a gradual increase in lipid accumulation from day 8 to day 28. The adipocytes displayed unilocular lipid droplets on days 18 and 28 (Fig. 2A).

The mean diameter of the adipocytes as assessed by the Coulter Multisizer III was 20.2 μm on day 8 and 37.5 μm on day 30 (Fig. 2B). During the course of adipocyte hypertrophy, ROS production increased 2.7-folds (day 18) and 4.3-folds (day 28) in comparison with the levels on day 8 (Fig. 2C). The mRNA and protein levels of MCP-1 and IL-6 were elevated substantially on days 18 and 28 (Fig. 2D and E, respectively). The AGT mRNA level was significantly lower on days 18 (48%) and 28 (42%) than that on day 8 (Fig. 2D). The AGT concentration in the culture media was decreased on days 18 (59% of the initial value) and 28 (42% of the initial value) (Fig. 2E). These results suggest that AGT expression and secretion were decreased in the hypertrophied adipocytes.

3.3. Impact of TNFα on the expression and secretion of AGT in adipocytes

Tumor necrosis factor α plays a critical role in the pathophysiology of inflammation and oxidative stress [27,34,35]. To explore the impact of TNFα on the expression and secretion of AGT in adipocytes, the differentiated 3T3-L1 adipocytes (day 8) were treated with TNFα (Sigma-Aldrich Japan) for 24 hours. Treatment with TNFα decreased the AGT mRNA level in a dose-dependent manner along with a concomitant increase in the MCP-1 and IL-6 mRNA levels (Fig. 3A). The AGT protein level in the culture media decreased in parallel to the AGT mRNA level (Fig. 3B).

We also investigated the effects of TNFα on primary adipocytes. Similarly to 3T3-L1 adipocytes, treatment with TNFα (10 ng/mL) for 24 hours slightly but significantly decreased AGT mRNA level and substantially increased MCP-1 mRNA level (Fig. 3C).

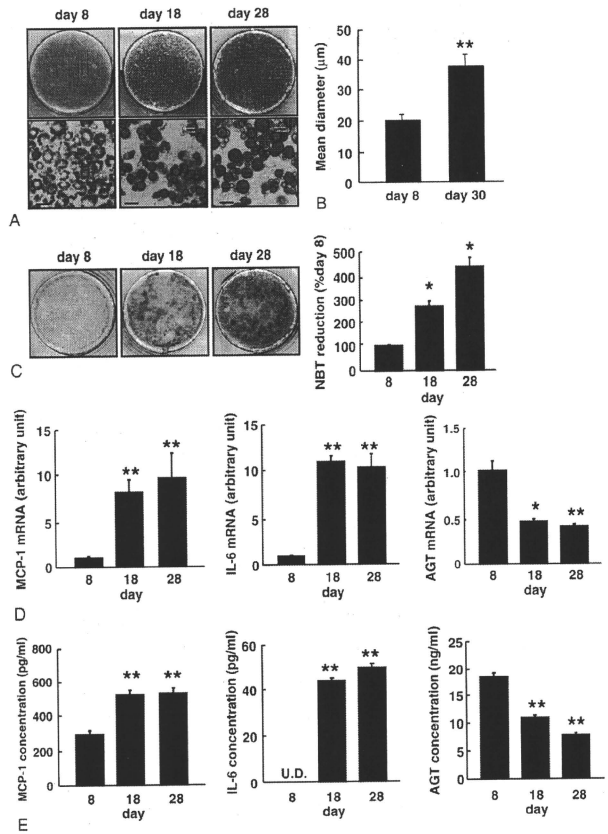

Fig. 2. The AGT expression during the course of hypertrophy in the 3T3-L1 adipocytes. A, Oil red O staining of the 3T3-L1 adipocytes on days 8, 18, and 28 after induction of differentiation. Bar = 30 μm. B, Size of the 3T3-L1 adipocytes on days 8 and 30. Adipocyte size was measured using a Coulter Multisizer III. C, The ROS production during adipocyte hypertrophy. The ROS production was assessed by the NBT assay. Dark blue formazan was dissolved, and the absorbance was determined at 560 nm (n = 3). D, The MCP-1, IL-6, and AGT mRNA levels in the 3T3-L1 adipocytes on days 8, 18, and 28 (n = 4). The mRNA level was examined by real-time PCR and normalized to that of 18S rRNA. E, The AGT protein concentration in the culture media. The MCP-1, IL-6, and AGT concentrations in the 3T3-L1 adipocytes on days 8, 18, and 28 were analyzed by ELISA (n = 4). Results are representatives of at least 3 independent experiments. The data are expressed as the mean ± SE. $*P < .05$ and $**P < .01$ as compared with the value of day 8. U.D. indicates undetectable.

3.4. Impact of oxidative stress on the expression and secretion of AGT in adipocytes

To explore the impact of oxidative stress on the expression and secretion of AGT in adipocytes, differentiated 3T3-L1 adipocytes (day 8) were exposed to a specific ROS molecule, hydrogen peroxide (H_2O_2), for 24 hours [17,36]. Incubation of adipocytes with H_2O_2 significantly increased the MCP-1 mRNA level, consistent with a previous report [17]. In contrast, H_2O_2 diminished the AGT mRNA level up to 35% of the initial value in a dose-dependent manner (Fig. 4A). The AGT protein level in the

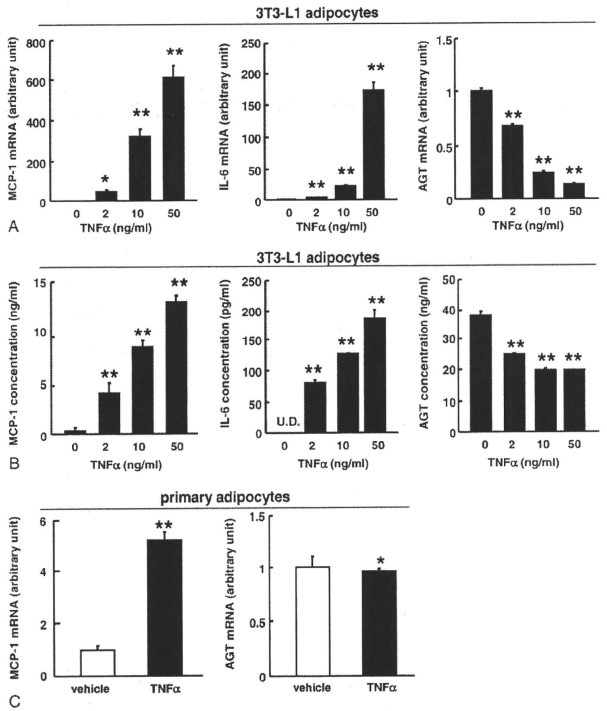

Fig. 3. Impact of TNFα on the expression and secretion of AGT in the 3T3-L1 adipocytes. A, The AGT, MCP-1, and IL-6 mRNA level in the 3T3-L1 adipocytes (day 8) treated with TNFα for 24 hours (n = 4). The mRNA level was examined by real-time PCR and normalized to that of 18S rRNA. B, The AGT protein concentration in the culture media in the 3T3-L1 adipocytes (day 8) treated with TNFα for 24 hours (n = 4). The protein level was assessed by ELISA. C, The AGT and MCP-1 mRNA level in the primary adipocytes treated with TNFα (10 ng/mL) for 24 hours (n = 4). The mRNA level was examined by real-time PCR and normalized to that of 18S rRNA. Results are representatives of at least 3 independent experiments. The data are expressed as the mean ± SE. $*P < .05$ and $**P < .01$ as compared with the control value.

culture media also decreased up to 23% of the initial value (Fig. 4B).

Similar to 3T3-L1 adipocytes, H_2O_2 treatment (1 mmol/L, 24 hours) significantly decreased AGT mRNA level in primary adipocytes (Fig. 4C). The H_2O_2 treatment tended to increase the MCP-1 mRNA level.

3.5. Effect of antioxidant treatment on the expression and secretion of AGT in adipocytes

We examined whether inhibition of ROS generation could nullify the decrease in AGT gene expression and AGT secretion in obese adipose tissue. First, we treated 3T3-L1 adipocytes with the antioxidant NAC (10 mmol/L) for 10 days (days 8-18). Without the NAC treatment, the adipocytes had become hypertrophic and increased ROS production in this period (Fig. 2B and C). The NBT assay revealed that NAC treatment significantly suppressed ROS production (Fig. 5A). Although ROS production was reported to potentiate adipocyte differentiation in early phase [37], the ROS suppression with the NAC treatment in our experiments did not cause morphologic changes in hypertrophied adipocytes compared with the vehicle treatment. The NAC treatment inhibited the increase in MCP-1 expression (Fig. 5B). The AGT mRNA level was significantly elevated with NAC treatment (Fig. 5B).

To test whether such phenomenon is reproducible in obese adipose tissue where ROS production is exaggerated

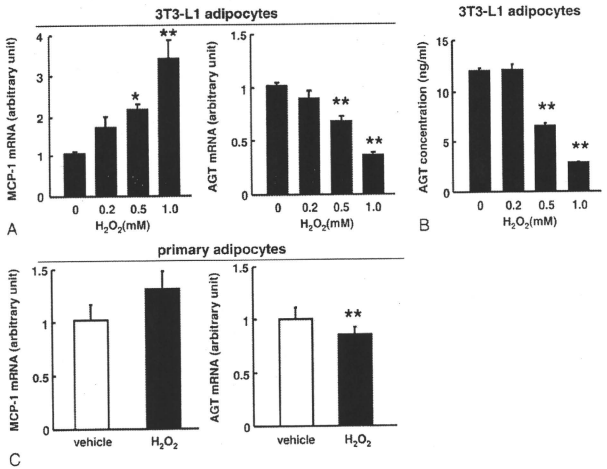

Fig. 4. Impact of oxidative stress on the expression and secretion of AGT in the 3T3-L1 adipocytes. A, The AGT and MCP-1 mRNA level in the 3T3-L1 adipocytes (day 8) treated with H_2O_2 for 24 hours (n = 4). The mRNA level was examined by real-time PCR and normalized to that of 18S rRNA. B, The AGT protein level in the culture media of the 3T3-L1 adipocytes (day 8) treated with H_2O_2 for 24 hours (n = 4). The protein concentration was assessed by ELISA. C, The AGT and MCP-1 mRNA level in the primary adipocytes treated with H_2O_2 (1 mmol/L) for 24 hours (n = 4). The mRNA level was examined by real-time PCR and normalized to that of 18S rRNA. Results are representatives of at least 3 independent experiments. The data are expressed as the mean ± SE. $^*P < .05$ and $^{**}P < .01$ as compared with the control value.

[17], we administered NAC to obese *db/db* mice once daily for 1 week. Similar to the obese *ob/ob* mice and DIO mice, in obese *db/db* mice (mean body weight, 48 ± 1.5 g), the AGT mRNA level in epididymal adipose tissue was markedly decreased to 22% as compared with their lean littermates (mean body weight, 28 ± 1.0 g) (Fig. 5C). In contrast, the TNFα mRNA level in epididymal adipose tissue was significantly higher in *db/db* mice than in their lean littermates (Fig. 5C). Both systemic and local (adipose tissue) oxidative stress was elevated substantially in obese *db/db* mice [38]. Notably, in *db/db* mice, NAC treatment significantly reduced the oxidative stress also in adipose tissue [38].

In the NAC treatment group, the AGT mRNA level in the epididymal adipose depots increased significantly by 2.1-folds compared with that in the vehicle group, whereas the IL-6 ($P = .052$) and TNFα ($P = .10$) mRNA levels tended to decrease in the NAC treatment group (Fig. 5D). On the other hand, the hepatic AGT mRNA level remained unchanged in both groups (Fig. 5E).

4. Discussion

The major finding of the present study is that oxidative stress dysregulates AGT in adipose tissue in obese humans and rodents. The AGT mRNA level was decreased in both obese adipose tissue and hypertrophied adipocytes, in which oxidative stress was exaggerated. Exposure of oxidative stress decreased AGT expression not only in the adipocyte cell line but also in primary adipocytes. The decrease in AGT expression was rescued by treatment with the antioxidant both in vivo and in vitro. Such obesity-associated changes in AGT in the adipose tissue were not observed in the liver.

The AGT regulation in obese adipose tissue has long been analyzed, but results were inconsistent [6,12,13]. We here demonstrated that the AGT mRNA level in adipose tissue was reduced in both obese humans and mice (Fig. 1). In obese mice, there seem to be no apparent depot-specific (subcutaneous and epididymal adipose depots) or strain-specific (*ob/ob*, *db/db*, and DIO mice) differences in the fall of AGT in adipose tissue. The AGT mRNA level was decreased also in hypertrophied 3T3-L1 adipocytes (Fig. 2). These results are consistent with a previous report using differentiation system of human adipocytes in primary culture, where the AGT mRNA level increased in differentiation process, but decreased in further culture process [39].

In previous experiments, several hormonal and metabolic changes associated with obesity influence AGT expression in adipocytes; however, due to species differences and experimental conditions, there are controversies around the results [39-42]. On the other hand, our results indicate that

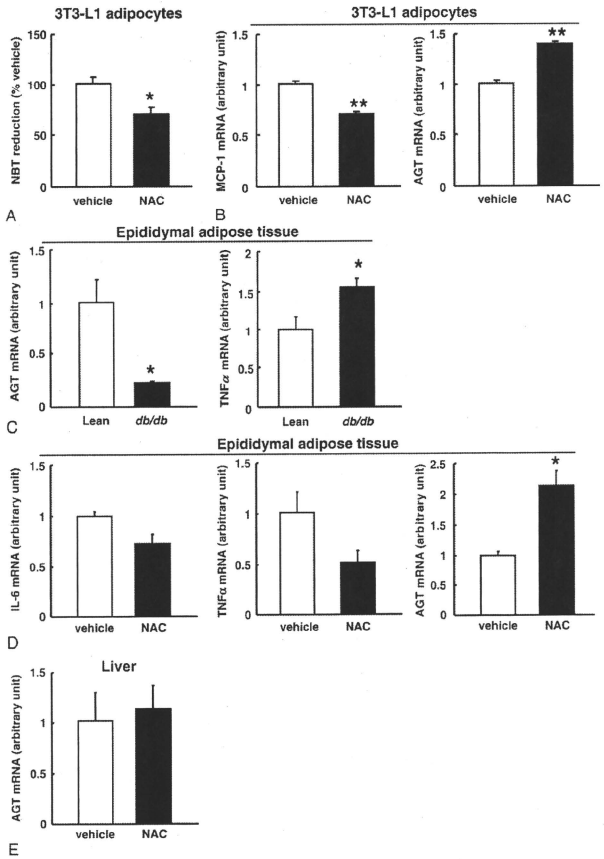

Fig. 5. Effect of antioxidant treatment on the expression and secretion of AGT in the adipocytes. A, Suppression of ROS generation in the 3T3-L1 adipocytes treated with NAC (10 mmol/L) for 10 days (n = 3). The ROS was estimated by the NBT assay. B, The MCP-1 and AGT mRNA levels in the 3T3-L1 adipocytes incubated with NAC (10 mmol/L) (n = 8). The mRNA level was examined by real-time PCR and normalized to that of 18S rRNA. Results are representatives of at least 3 independent experiments. C, Comparison of the AGT and TNFα mRNA levels between 10-week-old male *db/db* mice (n = 4; mean body weight, 48 ± 1.5 g) and their lean littermates (n = 4; mean body weight, 28 ± 1.0 g) in epididymal adipose tissue. D, The level of IL-6, TNFα, and AGT mRNA in the epididymal adipose tissue depots of obese *db/db* mice treated with NAC (150 mg/kg body weight) or vehicle (phosphate-buffered saline) once daily for 1 week (n = 3). E, The AGT mRNA level in the liver of obese *db/db* mice treated with NAC or vehicle for 1 week (n = 3). The mRNA level was examined by real-time PCR and normalized to that of cyclophilin mRNA. The data are expressed as the mean ± SE. $*P < .05$ and $**P < .01$ as compared with the control value.

AGT expression is decreased in obese adipose tissue. Reactive oxygen species (H_2O_2) decreased AGT expression in both 3T3-L1 adipocytes and primary adipocytes (Fig. 4). On the other hand, elimination of ROS with antioxidant increased AGT expression not only in hypertrophied 3T3-L1 adipocytes but also in adipose tissue from obese mice (Fig. 5). The oxidative stress–mediated decrease in adipose AGT is reproduced in our various experiments.

Several studies have suggested the augmentation of AGT by oxidative stress in the liver and kidney. In the liver, angiotensin II is known to enhance AGT expression via ROS generation [23], resulting in a positive feedback loop of AGT production [43]. In addition, oxidative stress mediated by hyperglycemia and hypertension has been shown to augment the expression of AGT in the rodent kidney [25,26]. In turn, elevated expression of AGT has been shown to activate renal RAS and considerably contribute to renal injury [26]. On the other hand, our data support a notion that oxidative stress "decreases" expression and secretion of AGT in obese adipose tissue, implying that regulation of AGT in adipose tissue may be distinct from other tissues in response to oxidative stress.

The clinical or pathophysiologic implications of decreased AGT in obese adipose tissue still remain unclear. Although further studies are warranted, the notion that adipose tissue RAS is involved in the control of adipogenesis and adipose tissue mass [44] tempts us to speculate that tissue-specific decrease of AGT in obese adipose tissue may serve as a defense against further exacerbation of adiposity. In obese adipose tissue, exaggerated oxidative stress affects the expression of a variety of genes [17]. Representatively, ROS induces the proinflammatory TNFα but suppresses the anti-inflammatory adiponectin in murine adipose tissue [17]. Glutathione peroxidase 3 (GPx3), an antioxidant enzyme secreted from the adipose tissue and kidney, is known to be decreased by oxidative stress exclusively in adipose tissue in obese *db/db* mice [38]. Notably, in vivo administration of an antioxidant was shown to rescue the decrease in GPx3 expression only in adipose tissue, but not in the kidney [38]. In this context, AGT shares close similarity with adiponectin and GPx3 in terms of the response to oxidative stress in adipose tissue.

Tissue-specific dysregulation of AGT has also been observed in inflammatory response [45,46]. Hepatic AGT is shown to increase by inflammatory stimuli via the acute-phase responsive element (APRE) on the promoter region of the AGT gene [43,47]. In rats treated with lipopolysaccharide, AGT mRNA level was shown to increase in the liver, aorta, and adrenal gland, but remained unchanged in the kidney [45]. Furthermore, in transgenic mice with cardioselective overexpression of TNFα, expression of AGT was decreased exclusively in the heart [46]. In the present study, we demonstrated that TNFα decreased the expression and secretion of AGT in 3T3-L1 adipocytes (Fig. 3). Considering that chronic, low-grade inflammation is a manifestation of obese adipose tissue [48,49], our results suggest that AGT is inversely regulated by inflammation in obese adipose tissue.

Previous works have raised a possibility that the inflammatory responses to AGT in adipose tissue and liver are controlled by distinct mechanisms [50]. In cultured adipocytes, inflammatory signals transcriptionally decrease AGT by the inhibition of APRE [50]; however, in cultured hepatocytes, nuclear factor–κB signaling augments AGT by the activation of APRE [47]. Importantly, the intracellular signaling involved in oxidative stress and inflammation interact and share, at least in part, common pathways in a tissue-specific manner [18,19]. In this context, tissue-specific dysregulation of AGT by oxidative stress is reminiscent of the case in inflammatory signals; and a possible link between the dysregulation of AGT and oxidative stress in obese adipose tissue may provide a fresh clue to dissect the pathophysiology of obesity. For example, we would suggest the one possibility that oxidative stress–induced suppression of adipose tissue RAS via the decrease in AGT may control adipose tissue function including adipocyte differentiation, lipolysis, and local blood flow [44].

In summary, the present study demonstrates for the first time that oxidative stress dysregulates AGT in obese adipose tissue in humans and rodents as well as in cultured adipocytes with hypertrophy. Our results support a concept that oxidative stress–dependent decrease in AGT may be a unique facet of dysfunction in obese adipose tissue.

Acknowledgment

We are grateful to A Katsurada (Departments of Medicine and Physiology, and Hypertension and Renal Center of Excellence, Tulane University Health Sciences Center, New Orleans, LA), M Tabuchi (Department of Pharmacology, Kinki University School of Medicine, Osaka-sayama, Japan), M Okada (Department of Internal Medicine, Kobe University Graduate School of Medicine, Kobe, Japan), and M Kasuga (Research Institute, International Medical Center of Japan, Tokyo, Japan) for help and discussion. We also thank A Ryu, S Maki, and M Nagamoto for assistance and Y Kobayashi and T Fukui for discussion.

This work was supported in part by Grants-in-Aid (MEXT, Japan) B2 and S2, Takeda Medical Research Foundation, Smoking Research Foundation, Lilly Research Foundation, Research on Measures for Intractable Diseases (Health and Labor Science Research Grant), Special Coordination Funds for Promoting Science and Technology (JST), Research Grant of National Cardiovascular Center, Sankyo Research Foundation, the Korea Research Foundation Grant (KRF-2008-005-J00203), and the National Research Laboratory Program (ROA-2004-000-10359-0) funded by the Korean Government.

References

[1] Engeli S. Role of the renin-angiotensin-aldosterone system in the metabolic syndrome. Contrib Nephrol 2006;151:122-34.
[2] Rahmouni K, Correia ML, Haynes WG, Mark AL. Obesity-associated hypertension: new insights into mechanisms. Hypertension 2005;45: 9-14.
[3] Dzau VJ. Circulating versus local renin-angiotensin system in cardiovascular homeostasis. Circulation 1988;77(6 Pt 2):I4-113.
[4] Raizada V, Skipper B, Luo W, Griffith J. Intracardiac and intrarenal renin-angiotensin systems: mechanisms of cardiovascular and renal effects. J Investig Med 2007;55:341-59.

[5] Cassis LA, Saye J, Peach MJ. Location and regulation of rat angiotensinogen messenger RNA. Hypertension 1988;11(6 Pt 2): 591-6.
[6] Giacchetti G, Faloia E, Mariniello B, Sardu C, Gatti C, Camilloni MA, et al. Overexpression of the renin-angiotensin system in human visceral adipose tissue in normal and overweight subjects. Am J Hypertens 2002;15:381-8.
[7] Engeli S, Negrel R, Sharma AM. Physiology and pathophysiology of the adipose tissue renin-angiotensin system. Hypertension 2000;35: 1270-7.
[8] Massiera F, Seydoux J, Geloen A, Quignard-Boulange A, Turban S, Saint-Marc P, et al. Angiotensinogen-deficient mice exhibit impairment of diet-induced weight gain with alteration in adipose tissue development and increased locomotor activity. Endocrinology 2001; 142:5220-5.
[9] Massiera F, Bloch-Faure M, Ceiler D, Murakami K, Fukamizu A, Gasc JM, et al. Adipose angiotensinogen is involved in adipose tissue growth and blood pressure regulation. FASEB J 2001;15:2727-9.
[10] Frederich Jr RC, Kahn BB, Peach MJ, Flier JS. Tissue-specific nutritional regulation of angiotensinogen in adipose tissue. Hypertension 1992;19:339-44.
[11] Boustany CM, Bharadwaj K, Daugherty A, Brown DR, Randall DC, Cassis LA. Activation of the systemic and adipose renin-angiotensin system in rats with diet-induced obesity and hypertension. Am J Physiol Regul Integr Comp Physiol 2004;287:R943-9.
[12] Van Harmelen V, Ariapart P, Hoffstedt J, Lundkvist I, Bringman S, Arner P. Increased adipose angiotensinogen gene expression in human obesity. Obes Res 2000;8:337-41.
[13] Engeli S, Bohnke J, Gorzelniak K, Janke J, Schling P, Bader M, et al. Weight loss and the renin-angiotensin-aldosterone system. Hypertension 2005;45:356-62.
[14] Engeli S, Schling P, Gorzelniak K, Boschmann M, Janke J, Ailhaud G, et al. The adipose-tissue renin-angiotensin-aldosterone system: role in the metabolic syndrome? Int J Biochem Cell Biol 2003;35:807-25.
[15] Keaney Jr JF, Larson MG, Vasan RS, Wilson PW, Lipinska I, Corey D, et al. Obesity and systemic oxidative stress: clinical correlates of oxidative stress in the Framingham Study. Arterioscler Thromb Vasc Biol 2003;23:434-9.
[16] Urakawa H, Katsuki A, Sumida Y, Gabazza EC, Murashima S, Morioka K, et al. Oxidative stress is associated with adiposity and insulin resistance in men. J Clin Endocrinol Metab 2003;88:4673-6.
[17] Furukawa S, Fujita T, Shimabukuro M, Iwaki M, Yamada Y, Nakajima Y, et al. Increased oxidative stress in obesity and its impact on metabolic syndrome. J Clin Invest 2004;114:1752-61.
[18] Stocker R, Keaney Jr JF. Role of oxidative modifications in atherosclerosis. Physiol Rev 2004;84:1381-478.
[19] Grattagliano I, Palmieri VO, Portincasa P, Moschetta A, Palasciano G. Oxidative stress–induced risk factors associated with the metabolic syndrome: a unifying hypothesis. J Nutr Biochem 2008;19:491-504.
[20] Griendling KK, Minieri CA, Ollerenshaw JD, Alexander RW. Angiotensin II stimulates NADH and NADPH oxidase activity in cultured vascular smooth muscle cells. Circ Res 1994;74:1141-8.
[21] Das DK, Maulik N, Engelman RM. Redox regulation of angiotensin II signaling in the heart. J Cell Mol Med 2004;8:144-52.
[22] Sachse A, Wolf G. Angiotensin II–induced reactive oxygen species and the kidney. J Am Soc Nephrol 2007;18:2439-46.
[23] Brasier AR, Jamaluddin M, Han Y, Patterson C, Runge MS. Angiotensin II induces gene transcription through cell-type–dependent effects on the nuclear factor–kappaB (NF-kappaB) transcription factor. Mol Cell Biochem 2000;212:155-69.
[24] Hsieh TJ, Zhang SL, Filep JG, Tang SS, Ingelfinger JR, Chan JS. High glucose stimulates angiotensinogen gene expression via reactive oxygen species generation in rat kidney proximal tubular cells. Endocrinology 2002;143:2975-85.
[25] Brezniceanu ML, Liu F, Wei CC, Tran S, Sachetelli S, Zhang SL, et al. Catalase overexpression attenuates angiotensinogen expression and apoptosis in diabetic mice. Kidney Int 2007;71:912-23.
[26] Miyata K, Ohashi N, Suzaki Y, Katsurada A, Kobori H. Sequential activation of the reactive oxygen species/angiotensinogen/renin-angiotensin system axis in renal injury of type 2 diabetic rats. Clin Exp Pharmacol Physiol 2008;35:922-7.
[27] Houstis N, Rosen ED, Lander ES. Reactive oxygen species have a causal role in multiple forms of insulin resistance. Nature 2006;440:944-8.
[28] Frost SC, Lane MD. Evidence for the involvement of vicinal sulfhydryl groups in insulin-activated hexose transport by 3T3-L1 adipocytes. J Biol Chem 1985;260:2646-52.
[29] Fujimoto M, Masuzaki H, Tanaka T, Yasue S, Tomita T, Okazawa K, et al. An angiotensin II AT1 receptor antagonist, telmisartan augments glucose uptake and GLUT4 protein expression in 3T3-L1 adipocytes. FEBS Lett 2004;576:492-7.
[30] Sakai T, Sakaue H, Nakamura T, Okada M, Matsuki Y, Watanabe E, et al. Skp2 controls adipocyte proliferation during the development of obesity. J Biol Chem 2007;282:2038-46.
[31] Kobori H, Katsurada A, Miyata K, Ohashi N, Satou R, Saito T, et al. Determination of plasma and urinary angiotensinogen levels in rodents by newly developed ELISA. Am J Physiol Renal Physiol 2008;294: F1257-63.
[32] Oliveira HR, Verlengia R, Carvalho CR, Britto LR, Curi R, Carpinelli AR. Pancreatic beta-cells express phagocyte-like NAD(P)H oxidase. Diabetes 2003;52:1457-63.
[33] Saye JA, Cassis LA, Sturgill TW, Lynch KR, Peach MJ. Angiotensinogen gene expression in 3T3-L1 cells. Am J Physiol 1989;256(2 Pt 1): C448-51.
[34] Wajant H, Pfizenmaier K, Scheurich P. Tumor necrosis factor signaling. Cell Death Differ 2003;10:45-65.
[35] Cawthorn WP, Sethi JK. TNF-alpha and adipocyte biology. FEBS Lett 2008;582:117-31.
[36] Kamigaki M, Sakaue S, Tsujino I, Ohira H, Ikeda D, Itoh N, et al. Oxidative stress provokes atherogenic changes in adipokine gene expression in 3T3-L1 adipocytes. Biochem Biophys Res Commun 2006;339:624-32.
[37] Lee H, Lee YJ, Choi H, Ko EH, Kim JW. Reactive oxygen species facilitate adipocyte differentiation by accelerating mitotic clonal expansion. J Biol Chem 2009;284:10601-9.
[38] Lee YS, Kim AY, Choi JW, Kim M, Yasue S, Son HJ, et al. Dysregulation of adipose glutathione peroxidase 3 in obesity contributes to local and systemic oxidative stress. Mol Endocrinol 2008;22:2176-89.
[39] Wang B, Jenkins JR, Trayhurn P. Expression and secretion of inflammation-related adipokines by human adipocytes differentiated in culture: integrated response to TNF-alpha. Am J Physiol Endocrinol Metab 2005;288:E731-40.
[40] Jones BH, Standridge MK, Taylor JW, Moustaid N. Angiotensinogen gene expression in adipose tissue: analysis of obese models and hormonal and nutritional control. Am J Physiol 1997;273(1 Pt 2): R236-42.
[41] Aubert J, Safonova I, Negrel R, Ailhaud G. Insulin down-regulates angiotensinogen gene expression and angiotensinogen secretion in cultured adipose cells. Biochem Biophys Res Commun 1998;250: 77-82.
[42] Harte A, McTernan P, Chetty R, Coppack S, Katz J, Smith S, et al. Insulin-mediated upregulation of the renin angiotensin system in human subcutaneous adipocytes is reduced by rosiglitazone. Circulation 2005;111:1954-61.
[43] Morgan L, Broughton Pipkin F, Kalsheker N. Angiotensinogen: molecular biology, biochemistry and physiology. Int J Biochem Cell Biol 1996;28:1211-22.
[44] Thatcher S, Yiannikouris F, Gupte M, Cassis L. The adipose renin-angiotensin system: role in cardiovascular disease. Mol Cell Endocrinol 2009;302:111-7.
[45] Nyui N, Tamura K, Yamaguchi S, Nakamaru M, Ishigami T, Yabana M, et al. Tissue angiotensinogen gene expression induced by lipopolysaccharide in hypertensive rats. Hypertension 1997;30: 859-67.

[46] Flesch M, Hoper A, Dell'Italia L, Evans K, Bond R, Peshock R, et al. Activation and functional significance of the renin-angiotensin system in mice with cardiac restricted overexpression of tumor necrosis factor. Circulation 2003;108:598-604.

[47] Ron D, Brasier AR, Habener JF. Transcriptional regulation of hepatic angiotensinogen gene expression by the acute-phase response. Mol Cell Endocrinol 1990;74:C97-C104.

[48] Hotamisligil GS, Arner P, Caro JF, Atkinson RL, Spiegelman BM. Increased adipose tissue expression of tumor necrosis factor–alpha in human obesity and insulin resistance. J Clin Invest 1995;95: 2409-15.

[49] Xu H, Barnes GT, Yang Q, Tan G, Yang D, Chou CJ, et al. Chronic inflammation in fat plays a crucial role in the development of obesity-related insulin resistance. J Clin Invest 2003;112:1821-30.

[50] Ron D, Brasier AR, McGehee Jr RE, Habener JF. Tumor necrosis factor–induced reversal of adipocytic phenotype of 3T3-L1 cells is preceded by a loss of nuclear CCAAT/enhancer binding protein (C/EBP). J Clin Invest 1992;89:223-33.

Relevant use of Klotho in FGF19 subfamily signaling system in vivo

Ken-ichi Tomiyama[a,b,1], Ryota Maeda[a,b,1], Itaru Urakawa[c], Yuji Yamazaki[c], Tomohiro Tanaka[a,b], Shinji Ito[a,b], Yoko Nabeshima[a,b], Tsutomu Tomita[d], Shinji Odori[d], Kiminori Hosoda[d], Kazuwa Nakao[d], Akihiro Imura[a,b], and Yo-ichi Nabeshima[a,b,2]

[a]Department of Pathology and Tumor Biology, Graduate School of Medicine, Kyoto University, Sakyo-Ku, Kyoto 606-8501, Japan; [c]Pharmaceutical Research Laboratories, Kyowa Hakko Kirin Company, Ltd., Takasaki, Gunma 370-1295, Japan; [b]Core Research for Evolutional Science and Technology, Japan Science and Technology Corporation, Kawaguchi-shi, Saitama 332-0012, Japan; and [d]Department of Medicine and Clinical Science, Graduate School of Medicine, Kyoto University, Sakyo-Ku, Kyoto 606-8501, Japan

Communicated by Yoshito Kaziro, Kyoto University, School of Medicine, Kyoto, Japan, December 9, 2009 (received for review September 28, 2009)

α-Klotho (α-Kl) and its homolog, β-Klotho (β-Kl) are key regulators of mineral homeostasis and bile acid/cholesterol metabolism, respectively. FGF15/ humanFGF19, FGF21, and FGF23, members of the FGF19 subfamily, are believed to act as circulating metabolic regulators. Analyses of functional interactions between α- and β-Kl and FGF19 factors in wild-type, *α-kl*$^{-/-}$, and *β-kl*$^{-/-}$ mice revealed a comprehensive regulatory scheme of mineral homeostasis involving the mutually regulated positive/negative feedback actions of α-Kl, FGF23, and 1,25(OH)$_2$D and an analogous regulatory network composed of β-Kl, FGF15/humanFGF19, and bile acids that regulate bile acid/cholesterol metabolism. Contrary to in vitro data, β-Kl is not essential for FGF21 signaling in adipose tissues in vivo, because (*i*) FGF21 signals are transduced in the absence of β-Kl, (*ii*) FGF21 could not be precipitated by β-Kl, and (*iii*) essential phenotypes in *Fgf21*$^{-/-}$ mice (decreased expressions of *Hsl* and *Atgl* in WAT) were not replicated in *β-kl*$^{-/-}$ mice. These findings suggest the existence of Klotho-independent FGF21 signaling pathway(s) where undefined cofactors are involved. One-to-one functional interactions such as α-Klotho/ FGF23, β-Klotho/FGF15 (humanFGF19), and undefined cofactor/ FGF21 would result in tissue-specific signal transduction of the FGF19 subfamily.

bile acid | cholesterol | mineral homeostasis | Cyp genes | energy source

The physiological roles of the Klotho family have remained puzzling since the original mutant mouse was developed (1). α-Kl deficiency in mice led to a characteristic phenotype resembling premature aging symptoms in human (1). Thereafter, we found that the overproduction of 1,25(OH)$_2$D and altered mineral-ion homeostasis are the major cause of these premature aging-like phenotypes observed in *α-kl*$^{-/-}$ mice, because the lowering of 1,25(OH)$_2$D activity by dietary restriction (a regimen in which *α-kl*$^{-/-}$ mice are fed a vitamin D–deficient diet) (2) is able to rescue the premature aging–like phenotypes and enable *α-kl*–deficient mice to survive normally without obvious abnormalities. Recently we have reported that α-Kl interacts with fibroblast growth factor 23 (FGF23) in kidney and plays an essential role in maintaining serum 1,25(OH)$_2$D levels by regulation of key active vitamin D–metabolizing enzymes, 1α-hydroxylase (Cyp27b1), and 24-hydroxylalse (Cyp24) (3). We also found that α-Kl binds to Na^+,K^+-ATPase in choroid plexus, parathyroid glands, and the distal convoluted tubules (DCT) of the kidney where extracellular calcium concentration is coordinately regulated (4). In these tissues, Na^+,K^+-ATPase activity is controlled in an α-Kl–dependent manner for transepithelial calcium transport in the choroid plexus and DCT, and for regulated PTH secretion in the parathyroid glands. By associating with both Na^+,K^+-ATPase and circulating FGF23, α-Kl plays a multifunctional role in α-Kl expressing tissues to regulate calcium and phosphate concentrations in vivo. This led to the concept that α-Kl is a regulator that integrates mineral homeostasis (5).

We next identified *β-kl*, which shares structural identity and characteristics with *α-kl* (6). β-Kl is predominantly expressed in the liver, pancreas, and adipose tissues (6) distinct from α-Kl expressing tissues (1, 2). To understand the biological role(s) of β-Kl, we generated a mouse line lacking *β-kl* (7). Although there were no gross abnormalities in the appearance of *β-kl*$^{-/-}$ mice, these mice exhibited an altered metabolism of bile acids, a group of structurally diverse molecules that are primarily synthesized in the liver from cholesterol, promote absorption of dietary lipids in the intestine, and stimulate biliary excretion of cholesterol (8). The enterohepatic circulation of bile acids is regulated largely in hepatocytes where bile acid biosynthesis is regulated by rate-limiting enzymes; cholesterol 7α-hydroxylase (Cyp7a1) and sterol 12α-hydroxylase (Cyp8b1) (8). Bile acids and oxysterols act as ligands to nuclear receptors regulating the expression of important genes in cholesterol homeostasis (9). Particularly, bile acids bind to the promoter region of the farnesoid X receptor (FXR), which induces transcription of small heterodimer partner (SHP), a negative regulator of Cyp7a1 and Cyp8b1, resulting in suppression of bile acids synthesis in a negative feedback manner (9).

Simultaneously, Inagaki et al. reported that FGF15 dramatically suppresses expression of Cyp7a1 through a gut–liver signaling pathway that is different from the FXR/SHP-mediated negative feedback system (10). Moreover, the association of bile acids with FXR leads to the increase of *Fgf15* expression in intestine, resulting in repression of Cyp7a1 in the liver. Importantly, this negative feedback effect was not observed in *Fgf15*$^{-/-}$ and *Fgfr4*$^{-/-}$ mice, and highlighted a concept that the binding of FGF15 with FGFR4 is involved in a second negative feedback system in bile acid metabolism. Taken together, analogous to the role of α-Kl in FGF23/FGFR1-mediated signal transduction, it was hypothesized that β-Kl plays a critical role in FGF15/FGFR4 mediated negative feedback regulation of *Cyp7a1* and *Cyp8b1* expression in the liver (11).

The mammalian FGF family currently consists of 22 members subdivided into seven subfamilies based on their structural similarity and modes of action (12). Most FGFs play an important role as paracrine factors regulating cell growth, regeneration, differentiation, and morphogenesis (13). However, it has been established that members of the FGF-19 subfamily, which also includes FGF21 and FGF23, differ in two important aspects from other FGF proteins. First, they have no or very small mitotic

Author contributions: Y.-i.N. designed research; K.-i.T., R.M., I.U., Y.Y., T. Tanaka, S.I., Y.N., and S.O. performed research; T. Tomita, K.H., K.N., and A.I. analyzed data; and A.I. and Y.-i.N. wrote the paper.

The authors declare no conflict of interest.

Freely available online through the PNAS open access option.

[1]K.-i.T. and R.M. contributed equally to this work.

[2]To whom correspondence should be addressed. E-mail: nabemr@lmls.med.kyoto-u.ac.jp.

This article contains supporting information online at www.pnas.org/cgi/content/full/0913986107/DCSupplemental.

www.pnas.org/cgi/doi/10.1073/pnas.0913986107

effects; and second, they exert their action via systemic, hormone-like effects as metabolic regulators. In fact, human FGF19 (hFGF19) and its murine ortholog FGF15, as well as FGF23, are secreted from ileal enterocytes and bone, respectively, and then circulate in the bloodstream to target tissues (12–14). The third member, FGF21 is predominantly synthesized in the liver (15) and has beneficial effects on several metabolic parameters in different animal models of obesity; recently, FGF21 has been postulated to be a newly found regulator of glucose metabolism through induction of glucose transporter 1 (GLUT 1) (16).

As first shown for FGF23 and subsequently for FGF19, FGF21 has been predicted to require a specific cofactor for its binding to a certain type of FGFR and subsequent activation of FGF21/FGFR signaling pathway. β-Kl has been reported as a candidate cofactor essential for bioactivity of FGF21 in in vitro studies (16–22). However, these have not been confirmed in in vivo studies. It is particularly important to examine (*i*) whether FGF21 signal transduction is abolished in *β-kl*$^{-/-}$ mice and (*ii*) whether the phenotypes of *β-kl*$^{-/-}$ mice significantly overlap with those of *Fgf21*-deficient mice (*Fgf21*$^{-/-}$) (23, 24).

Recent advances in understanding the signaling of FGF19 subfamilies have mainly been based on conventional in vitro experiments (13, 17, 19, 22), whereas in vivo verification of the association of FGF ligands and FGF receptor or of FGF ligands and Klotho family proteins, as well as the signal transduction (phosphorylation) cascades triggered by FGF 19 subfamilies have yet to be confirmed.

In the present study, we demonstrate the first manifest evidence revealing that whereas α-Kl and β-Kl are required for FGF23 and FGF15/hFGF19-mediated signaling pathways in vivo, respectively, β-Kl appears not to be essential for FGF21-mediated signal transduction in vivo.

Results

α-Kl–Dependent Vitamin D Regulation by FGF23. FGF23 is derived from bone and is essential for maintaining phosphate homeostasis and regulation of vitamin D metabolism. In WT mice, administration of hFGF23 results in remarkable suppression of serum 1,25-dihydroxyvitamin D [1,25$(OH)_2$D] through the repression of *Cyp27b1* and induction of *Cyp24* in the kidney. As we previously reported, serum concentrations of 1,25$(OH)_2$D in both *α-kl*$^{-/-}$ and *Fgf23*$^{-/-}$ mice were remarkably higher than that of WT mice (2, 25). Intriguingly, serum FGF23 in *α-kl*$^{-/-}$ mice was >8,000-fold that of WT mice (Fig. 1*A*). To analyze how α-Kl and FGF23 coordinately regulate vitamin D metabolism in the kidney, we analyzed the interactive actions of FGF23 and α-Kl in vivo. The FGFs used in these experiments (hFGF23, hFGF19, hFGF21) were prepared from CHO cell culture media, and their activities were estimated by measuring *Egr-1*-promotor directed Luciferase activities using Peak rapid cells with or without exogenous expression of *α-kl* or *β-kl* (Fig. S1). Furthermore the activity of hFGF21 was confirmed by up-regulation of *Glut1* mRNA in 3T3-L1 adipocyte. To minimize the effects of hypervitaminosis D, a major cause of the abnormalities observed in *α-kl*$^{-/-}$ mice, we used *α-kl*$^{-/-}$ mice fed with a vitamin D–deficient diet, in which serum 1,25$(OH)_2$D levels were normal and consequently most of the premature aging–like phenotypes were alleviated (2).

hFGF23 administration induced a significant decrease in serum 1,25$(OH)_2$D levels in WT mice, whereas no effect was observed in *α-kl*$^{-/-}$ mice (Fig. 1*B*). Consistently, in WT kidneys injected with hFGF23, *Cyp27b1* expression was reduced >13-fold, whereas *Cyp24* expression was induced >5-fold (Fig. 1 *C* and *D*). However, no significant effect of hFGF23 was found on the expression of *Cyp27b1* and *Cyp24* in *α-kl*$^{-/-}$ mice. These results offer direct evidence that α-Kl is essential for FGF23-derived repression of *Cyp27b1* and induction of *Cyp24* in vivo. In addition, we found that the administration of hFGF23 resulted in down-regulation of α-Kl expression (Fig. 1*E*), probably because α-Kl is a target of FGF23 signal transduction and/or because of a secondary effect of decreased 1,25$(OH)_2$D, an inducer of α-Kl gene expression (2). These data implicate an elaborate mutual negative feedback system composed of α-Kl, FGF23, and 1,25$(OH)_2$D in mineral-ion maintenance (Fig. 5*A*).

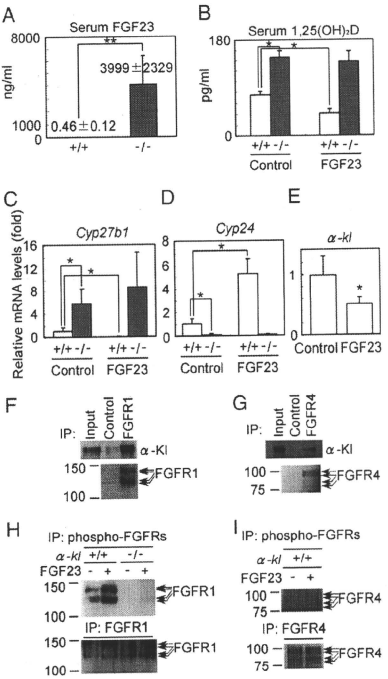

Fig. 1. FGF23 is dependent on α-Kl for regulation of vitamin D synthesis in kidney (*A–E*). (*A*) Serum concentrations of FGF23 in WT and *α-kl*$^{-/-}$ were measured by ELISA. WT (*open bars*) and *α-kl*$^{-/-}$ (*filled bars*) mice (n = 4/group) were injected with recombinant hFGF23 (0.2 mg/kg) or PBS control. Mice were killed 4 h after injection, and serum concentrations of 1,25$(OH)_2$D (*B*) were measured. *Cyp27b1* (*C*), *Cyp24* (*D*), and *α-kl* (*E*) mRNA levels in kidney were analyzed by RT–quantitative PCR. In this and all other figures, error bars represent mean ± SD and are plotted as fold change. Data were derived from 8- to 10-week-old male mice on vitamin D–deficient diets. *$P < 0.05$; **$P < 0.01$. FGFR1 binds to α-Kl and is phosphorylated by FGF23 in the kidney (*F–I*). (*F*) Kidney lysates were precipitated with anti-FGFR1 antibody or with control IgG. Input is 0.01% of the kidney whole extract used for the immunoprecipitation. (*G*) Kidney lysates were precipitated with anti-FGFR4 antibody or with control IgG. Input is 0.2% of the kidney whole extract used for the immunoprecipitation. (*H*) The kidney lysates of WT and *α-kl*$^{-/-}$ mice were immunoprecipitated with the anti-phospho-FGFRs or the anti-FGFR1 antibody. The immunoprecipitates were separated by SDS/PAGE and blotted with anti-FGFR1 antibody. (*I*) Kidney lysates of WT mice were immunoprecipitated with the anti–phospho-FGFRs or the anti-FGFR4 antibody and then blotted with anti-FGFR4 antibody.

α-Kl–Dependent FGFR1 Phosphorylation by FGF23 in Vivo. Generally FGFs can bind to and activate cell surface tyrosine kinase FGF receptors and transduce signals to downstream molecules including MAP kinase (26). The FGF receptor family consists of

four members, FGFR1–4. With the exception of FGFR4, splicing variants in the third Ig-like domain (IIIb and IIIc types) have been identified for each member (12, 26). Recently, it has been reported that α-Kl binds to FGFRs in cultured cells (19) and converts the canonical FGFR1(III)c to a receptor specific for FGF23 (3). We therefore tested whether the above observations were valid in vivo. We first examined the interactions between α-Kl and FGFR1, and α-Kl and FGFR4 in the kidney. As observed in in vitro experiments, α-Kl was coprecipitated not only with FGFR1 but also with FGFR4 in the kidney (Fig. 1*F* and *G*). We then investigated whether these two receptors are activated by hFGF23 in the kidney (procedures are as in *SI Text* and Fig. S2). In WT mice, FGFR1 was activated in the kidney 10 min after injection of hFGF23 (Fig. 1*H*). In contrast, phosphorylation of FGFR4 was not detectable even after the injection of hFGF23 (Fig. 1*I*), suggesting that FGFR4 is not a major receptor responsible for FGF23 signaling in the kidney. As expected, we could not detect phosphorylation of FGFR1 in the kidney of α-$kl^{-/-}$ mice even after hFGF23 injection (Fig. 1*H*). In summary, we concluded that FGFR1 is preferentially activated by FGF23 in a α-Kl–dependent manner in the kidney.

β-Kl–Dependent Bile Acid Regulation by FGF15. Because the unusually elevated expression of Cyp7a1 was observed not only in β-$kl^{-/-}$ mice (7) but also in *Fgf15*$^{-/-}$ and *Fgfr4*$^{-/-}$ mice (10, 27), we predicted that β-Kl was involved in FGF15/FGFR4-signaling system. Based on studies in cultured cells, it was recently proposed that β-Kl is necessary for FGF15/hFGF19-mediated signal transduction in the liver (18, 22). To confirm this hypothesis in vivo, we first measured the mRNA levels of *Fgf15* in the terminal ileum of WT and β-$kl^{-/-}$ mice. Interestingly, *Fgf15* expression levels were ~12-fold increased in β-$kl^{-/-}$ mice compared with those of WT (Fig. 2*A*), analogous to the elevation of FGF23 expression in α-$kl^{-/-}$ mice (Fig. 1*A*). To evaluate the effect of FGF15 in vivo, we administered hFGF19 and analyzed *Cyp7a1* and *Cyp8b1* expression. In WT mice, the expression levels of *Cyp7a1* and *Cyp8b1* 6 h after hFGF19 injection resulted in >100-fold and >10-fold reductions, respectively (Fig. 2 *B* and *C*). These were comparable to findings in a previous study examining FGF15 (10), and thus we concluded hFGF19 could be used to evaluate bile acid regulation in mice. In contrast, the expression levels of *Cyp7a1* and *Cyp8b1* remained elevated in β-$kl^{-/-}$ livers even after the administration of hFGF19 (Fig. 2 *B* and *C*), demonstrating that β-Kl is essential for the negative regulation of Cyp7a1 and Cyp8b1 by FGF15/hFGF19 in vivo. β-Kl-regulated bile acid synthesis by FGF15/hFGF19 is further described in *SI* (Fig. S3).

β-Kl/FGFR4 Coexpression Is Required for FGF15 Signaling in Vivo. To monitor whether FGF15/hFGF19 signals are transduced in tissues other than the liver, we verified *Egr-1* (a zinc-finger transcription factor identified as an immediate-early gene induced by cellular stimulation) mRNA levels in β-Kl–expressing tissues (liver, adipose, pancreas, and salivary gland) as well as several β-Kl–nonexpressing tissues, since hFGF23 administration remarkably increased *Egr-1* expression and induced phosphorylation of 44/42 MAP kinase (ERK1/2) in the kidney where α-Kl is expressed (3). In WT liver, *Egr-1* expression level increased by >120-fold 30 min after hFGF19 administration compared with vehicle (Fig. 2*D*). With respect to other tissues, we observed a faint, but statistically significant *Egr-1* increase in pancreas (>5-fold) and in white adipose tissue (WAT) (~3-fold). Nonetheless, no remarkable changes were observed in other tissues including brown adipose tissue (BAT) and salivary gland despite β-Kl expression. As expected, in β-$kl^{-/-}$ mice injected with hFGF19, no significant induction of *Egr-1* was observed in any of the tissues evaluated (Fig. 2*D*), demonstrating that β-Kl is necessary but not sufficient for FGF15/hFGF19-mediated signal transduction. To address the question of why FGF15/hFGF19 signal is transduced in the liver, pancreas, and WAT, but not in BAT and salivary glands, we profiled the expression of various FGF receptors (FGFRs) in β-Kl–expressing tissues. As reported previously (10), FGFR4 is postulated to be the major receptor responsible for FGF15-mediated signal transduction in the liver. As for the pancreas and WAT, we did observe >2-fold and >6-fold lower *Fgfr4* expression compared with that in the liver, respectively. On the contrary, *Fgfr4* mRNA was not detected in the salivary glands and BAT (Fig. S4). Hence *Egr-1* up-regulation by hFGF19 could be observed in tissues where β-Kl and FGFR4 are coexpressed.

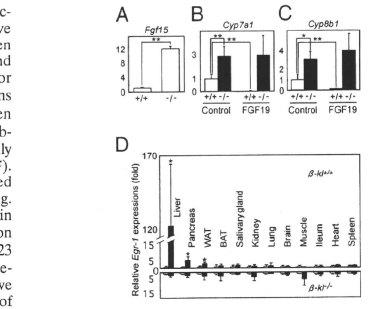

Fig. 2. FGF19 is dependent on β-Kl for regulation of bile acid synthesis in liver (*A–D*). (*A*) mRNA levels of *Fgf15* in terminal ileum in WT and β-$kl^{-/-}$ were measured by RTQ-PCR. WT mice (*open bars*) and β-$kl^{-/-}$ mice (*filled bars*) (n = 5/group) were injected with recombinant hFGF19 (1 mg/kg) or control medium. Mice were killed 6 h after injection and *Cyp7a1* (*B*) and *Cyp8b1* (*C*) mRNA levels in liver were measured by RT–quantitative PCR. Data were derived from 14- to 16-week-old male mice on standard diet. Egr-1 induction mediated by FGF19 in liver (*D*). hFGF19 (1 mg/kg) or control medium were injected into WT and β-$kl^{-/-}$ male mice (12–14 weeks old) on standard diet. Thirty minutes after injection, tissues in WT (*Upper*) and β-$kl^{-/-}$ (*Lower*) mice (n = 4/group) were excised. *Egr-1* mRNA levels were measured by RT-quantitative PCR. The expression levels of FGF19-injected mice (*filled bars*) and vehicle injected mice (*open bars*) are plotted as fold change. $^{*}P < 0.05$; $^{**}P < 0.01$.

To further demonstrate the contribution of β-Kl in the hepatic FGF15/hFGF19-mediated signaling cascade, we evaluated the phosphorylation of FGFR4 and downstream signaling molecules in vivo using the methods shown in Fig. 1 (Fig. S2 and *SI Text*). β-Kl could be efficiently precipitated by an anti-FGFR4 antibody (Fig. 3*A*) and the phosphorylation of FGFR4 was confirmed after hFGF19 treatment in WT liver (Fig. 3*B*). Unexpectedly, the amount of FGFR4 protein was significantly reduced in livers of β-$kl^{-/-}$ mice (Fig. 3*C*). To obtain an amount of FGFR4 equivalent to that obtained from WT mice, we concentrated the liver lysates from β-$kl^{-/-}$ mice and performed immunoprecipitation (Fig. S2 and *SI Text*). However, we could not detect enhanced activation of FGFR4 in β-$kl^{-/-}$ livers even after injection of hFGF19 (Fig. 3*D*). Consistent with a previous report (18), clear phosphorylation of ERK1/2 was observed in WT livers 10 min after hFGF19 injection, whereas it was undetectable in β-$kl^{-/-}$ livers (Fig. 3*E*), demonstrating that β-Kl is essential for the FGF15/hFGF19 directed activation of FGFR4 and downstream signaling cascade in the liver.

β-Kl Is Not Essential for FGF21-Mediated Signaling in Adipose Tissues. FGF21, a member of the FGF19 subfamily that is synthesized in the liver, has been reported to be a newly found regulator of glucose metabolism (16) and β-Kl has been postulated to be essential for its activity in in vitro studies (17, 20, 21). To examine the possible contribution of β-Kl in the FGF21 signaling system in vivo, we first administered recombinant hFGF21 to WT mice and analyzed *Egr-1* mRNA levels in multiple tissues (Fig. 4*A*). Before its use, we con-